LBL-28693
Preprint

Lawrence Berkeley Laboratory
UNIVERSITY OF CALIFORNIA

Submitted to Annals of Physics

A Thomas-Fermi Model of Nuclei
Part I: Formulation and First Results

W.D. Myers and W.J. Swiatecki

May 1990

LOAN COPY
Circulates
for 2 weeks
Bldg. 50 Library.
LBL-28693
Copy 2

Prepared for the U.S. Department of Energy under Contract Number DE-AC03-76SF00098.

DISCLAIMER

This document was prepared as an account of work sponsored by the United States Government. While this document is believed to contain correct information, neither the United States Government nor any agency thereof, nor the Regents of the University of California, nor any of their employees, makes any warranty, express or implied, or assumes any legal responsibility for the accuracy, completeness, or usefulness of any information, apparatus, product, or process disclosed, or represents that its use would not infringe privately owned rights. Reference herein to any specific commercial product, process, or service by its trade name, trademark, manufacturer, or otherwise, does not necessarily constitute or imply its endorsement, recommendation, or favoring by the United States Government or any agency thereof, or the Regents of the University of California. The views and opinions of authors expressed herein do not necessarily state or reflect those of the United States Government or any agency thereof or the Regents of the University of California.

LBL - 28693

A Thomas-Fermi Model of Nuclei
Part I: Formulation and First Results *

W.D. Myers and W.J. Swiatecki

Nuclear Science Division

Lawrence Berkeley Laboratory

1 Cyclotron Road

Berkeley, California 94720

*This work was supported by the Director, Office of Energy Research, Office of High Energy and Nuclear Physics, Nuclear Physics Division of the US Department of Energy under Contract DE - AC03 - 76SF00098.

Abstract

We formulate a Thomas-Fermi model of average nuclear properties (i.e. of nuclear masses, deformation energies, density distributions, optical model potentials, etc.) by generalizing the momentum dependent Seyler-Blanchard effective nucleon-nucleon interaction. In addition to reproducing the binding energy, density, symmetry energy and surface energy of nuclear matter, the generalized model can be adjusted to reproduce the diffuseness of the nuclear density distribution, as well as theoretical estimates of the binding properties of neutron matter. The depth of the nuclear optical potential, including its energy and isospin dependences, can also be reproduced. The above properties of nuclei and of neutron matter determine quite firmly the seven adjustable parameters of the theory, yielding a model that, apart from shell effects and the discreteness of nucleons, is expected to be accurate for very small or very deformed systems, and to be reliable for extrapolating to extremely large hypothetical nuclei, including systems with arbitrary neutron excess and arbitrary geometries,

such as those that sometimes arise in astrophysical applications. A preliminary set of the model's parameters has been determined, and one of the predictions of the theory is that the measured values of the nuclear surface energy and surface diffuseness, taken together, place a significant constraint on the value of the compressibility coefficient of standard nuclear matter. This constraint will provide a useful estimate of this quantity once the final set of parameters has been determined. The present paper is the first part in a comprehensive application of the model to conventional as well as exotic aspects of nuclear physics.

Contents

1 Introduction 6

2 The Effective Nucleon-Nucleon Interaction 9

3 The Thomas-Fermi Energy 18

4 Standard Nuclear Matter ($\rho_n = \rho_p$) 23

5 Uniform Nuclear Matter ($\rho_n \neq \rho_z$) 27

6 The Euler Equations 31

7 Semi-Infinite Distributions 36

8 Optical Model Potentials 41

9 Determination of a Preliminary Set of Interaction Parameters 51

10 The Truncated Thomas-Fermi Model 54

11 Summary and Outlook 57

12 Appendix A. The Interaction Energy 59

13 Appendix B. Numerical Solution of the Euler Equations. 68

14 Appendix C. Relation to Droplet Model Coefficients 70

15 Acknowledgements 72

1 Introduction

A two-part, macroscopic-microscopic treatment of the nuclear many-body problem has been widely exploited in the past 25 years. (For a review of this approach see, for example, Ref.[1].) The macroscopic part of such theories deals with smooth, statistical properties, to which estimates of microscopic shell effects are then added. The simplest macroscopic model is the four-parameter Liquid Drop approximation to a nucleus, according to which the specifically nuclear energy of N neutrons and Z protons, with $A = N + Z$, is a sum of volume and surface energies. For a given shape of the drop these energies are proportional to A and $A^{2/3}$, respectively, and they are assumed to be quadratic functions of the relative neutron excess $I = (N - Z)/(N + Z)$. An improved version of the Liquid Drop model, the Droplet Model [2,3], includes higher-order terms in an expansion in the small quantities $A^{-1/3}$ and I. This improvement is achieved at the price of additional adjustable parameters, the otherwise undetermined expansion coefficients. The Droplet Model has been quite useful in a variety of applications, but its limitations are also evident: The expansion in $A^{-1/3}$ fails for small or very deformed systems, and the expansion in I becomes progressively less reliable with increasing I,

for example for nuclei near the neutron drip line. Moreover, the number of adjustable parameters (nine in place of the original four) is both inconvenient and can lead to ambiguities, since the experimental data are insufficient to establish a firm parameter set.

It has been clear for some time that a statistical Thomas-Fermi model with an adjustable effective nucleon-nucleon interaction is a more nearly ideal macroscopic model [4–7]. It does not rely on expansions in $A^{-1/3}$ and I, and it is more efficient in its use of adjustable parameters. In its simplest form (the Seyler-Blanchard version with four parameters [2,8]), it can be adjusted to give a good account of the smooth trends of nuclear masses and sizes [9]. However, after this adjustment, no freedom is left to reproduce other known properties (such as the nuclear surface diffuseness or the nuclear optical potential) or to estimate unknown ones, such as the nuclear compressibility or the properties of neutron matter.

In the present paper we formulate a Thomas-Fermi model with a more flexible effective interaction and explore a specific version with six or, for some purposes, seven parameters [10]. This model should be capable of giving a very adequate description of average properties of all nuclei, including very light and very deformed systems, as well as nuclei near the drip lines. In

particular, the model can be used to estimate the nuclear compressibility and to throw light on the properties of neutron matter.

2 The Effective Nucleon-Nucleon Interaction

The nuclear Thomas-Fermi model is patterned on the atomic Thomas-Fermi approximation [5]. The total energy of the system is taken to be an integral over all space of a sum of kinetic and interaction energy densities. In the simplest approximation the former is proportional to the five-thirds power of the local particle density. The latter is the interaction energy density generated at a point by the surrounding particles through the agency of an appropriate law of force: the electrostatic interaction in the atomic case and an effective short-range interaction in the nuclear case. It is important to stress that the effective nuclear interaction must be able to reproduce, within the Thomas-Fermi approximation of dynamically uncorrelated particle motions, the saturating character of nuclear matter. This means that, in general, it must be velocity and/or density dependent. Thus, in contrast to the atomic case, one does not expect a correspondence between the effective interaction and the true particle-particle interaction in empty space. The effective interaction is, in fact, meant to mimic features of the nucleon-nucleon potential that cannot be treated in the Thomas-Fermi approximation (e.g. the anti-correlations due to a hard repulsive core) as well as the influence

of the nuclear medium on the binding properties of nucleons. As a result, the velocity dependence of the effective interaction does not bear any simple relation to the velocity dependence of nucleon-nucleon forces. As regards the density dependence of the effective interaction, such a concept cannot even be defined for particles interacting in empty space.

In what follows we shall take the effective nucleon-nucleon interactions to be both velocity and density dependent, and to have the following appearance:

$$v_{12} = v(r_{12}, p_{12}, \overline{\rho}) = -C f(r_{12}/a)\,, \tag{1}$$

where $f(r_{12}/a)$, a function of range a, specifies the dependence of the interaction on the distance r_{12} between the particles. (Thomas-Fermi models generalized to include a density dependent interaction have been considered before. See especially Ref.[5,11].) The interaction strength C consists of a constant modified by momentum-dependent and density-dependent terms, which we write as follows:

$$C = \frac{1}{2}(1 \mp \xi)\, C_\alpha - \frac{1}{2}(1 \mp \zeta)\left[C_\beta\, p_{12}^2 - C_\gamma\, p_{12}^{-1} + C_\sigma \overline{\rho}^{2/3}\right]. \tag{2}$$

Here p_{12} stands for the magnitude of the relative momentum of the interacting

particles and $\overline{\rho}$ is a mean density defined by

$$\overline{\rho}^{2/3} = \frac{1}{2}\left(\rho_1^{2/3} + \rho_2^{2/3}\right) , \tag{3}$$

where ρ_1 and ρ_2 are the relevant neutron or proton densities at points 1 and 2. Because of the proportionality of the Fermi energy to the two-thirds power of the density, $\overline{\rho}^{2/3}$ is proportional to a mean Fermi energy $\overline{T}$ defined by

$$\overline{T} = \frac{1}{2}\left(T_1 + T_2\right) , \tag{4}$$

where T_1 and T_2 are the relevant Fermi energies at the points 1 and 2.

The factors $\frac{1}{2}(1 \mp \xi)$ and $\frac{1}{2}(1 \mp \zeta)$ in Eq.(2) allow the interaction to be different for like and unlike pairs of particles. The minus sign refers to like (neutron-neutron or proton-proton) interactions, the plus sign to unlike (neutron-proton interactions). Altogether there are thus seven adjustable parameters: a, C_α, C_β, C_γ, C_σ, ξ and ζ. As will be seen in detail later, they play the following roles. The standard four-parameter Seyler-Blanchard model corresponds to eliminating three parameters by setting $C_\gamma = C_\sigma = 0$ and $\xi = \zeta$. The remaining four parameters can be used to fit four nuclear properties: the binding energy and density of nuclear matter, the nuclear symmetry energy coefficient and either the nuclear surface energy coefficient or the nuclear surface diffuseness. If the surface energy is fitted, the surface

diffuseness is fixed and comes out somewhat too small compared to measured values. The nuclear compressibility coefficient K is also fixed (at about 300 Mev), and there is no possibility of estimating its value by optimizing a fit to nuclear properties with respect to an adjustable parameter. The role of the fifth parameter C_γ is to provide such flexibility. As will be seen below, there is essentially a one-to-one relation between K and C_γ, and this allows an estimate of K to be made either by a fit of C_γ to nuclear masses or, even more directly, by fitting the nuclear surface diffuseness in addition to the surface energy. At this stage one has a flexible five-parameter model of nuclear binding energies and density distributions. A sixth parameter, associated with making ξ different from ζ, can be introduced in order to acquire the flexibility of varying the binding properties of *neutron* matter, while keeping the properties of familiar nuclear matter essentially fixed (and thus not affecting the fit to the bulk of measured nuclear masses).

The situation is still not quite satisfactory, however, if an additional body of data is brought into the discussion. Thus it turns out that in the above model the predicted velocity dependence of the potential felt by a nucleon moving in nuclear matter is intrinsically too strong to be consistent with data on neutron or proton scattering by nuclei, as interpreted by means of

an optical model potential [2,11]. In particular, the Thomas-Fermi model prediction would be that the optical potential should turn repulsive beyond about 70 MeV incident nucleon energy, in clear disagreement with measurements. This is a direct indication of the need for a density dependence of the effective interaction, which can then take over some of the burden of nuclear saturation from the velocity-dependent terms. With the seventh parameter C_σ added, the disagreement with the scattering data can be removed, and a seven-parameter Thomas-Fermi model in close correspondence with many nuclear properties is then available. As something of a bonus it will actually turn out that, for the discussion of binding energies and density distributions, the parameters C_β and C_σ always occur only in a particular combination C_B, say (see below), so that in describing masses and density distributions one is still dealing with a model with only *six* adjustable parameters: a, C_α, C_B, C_γ, ξ, and ζ. That is three fewer than in the standard Droplet Model and only two more than in the Liquid Drop Model.

As regards the particular choice of the momentum and density dependences given by Eq. (2), the following remarks are relevant. The term $C_\beta\, p_{12}^2$, familiar from Refs.[2,8], leads to a potential depth in nuclear matter which decreases parabolically with the momentum p of the particle in question.

Such a momentum-dependent repulsive effect provides a mechanism for nuclear saturation but, as pointed out above, a too rapid unbounded increase of the repulsion with p^2 can be an embarrassment when comparisons with scattering data are brought into the discussion. From this point of view the term $-C_\gamma\, p_{12}^{-1}$ leads to a more desirable dependence of the potential on the nucleon momentum p. Thus it turns out that for $p < P$, where P is the Fermi momentum of the surrounding medium, the decrease of the potential depth is also exactly parabolic, but for $p > P$ this changes to a p^{-1} dependence, the contribution of the C_γ-term thus tending to zero rather than infinity for large values of p. (The dependence on p parallels the dependence on distance of an electric potential that would be generated by a negative uniform charge density inside a sphere of radius P: parabolic inside, inverse-distance outside the sphere).

As mentioned earlier, the justification of a term like $C_\gamma\, p_{12}^{-1}$ is not to be sought in the properties of the nucleon-nucleon force in empty space but in the implied binding properties in nuclear matter (discussed later on and illustrated in Fig. 7). From a pragmatic point of view, the combination of $C_\beta\, p_{12}^2$ and $C_\gamma\, p_{12}^{-1}$ is simply a more flexible parameterization of the momentum- dependent saturating effects than the conventional term $C_\beta\, p_{12}^2$ alone. As will

be seen presently, the particular choice $C_\gamma\, p_{12}^{-1}$ results in a useful simplification of the algebraic structure of the equations governing the model. This is also true of the particular choice of the density dependence associated with the term $C_\sigma\, \overline{\rho}^{2/3}$.

It proves convenient to re-write the interaction strength C by introducing natural units of energy, density and momentum. Thus, given a set of force parameters, imagine the equilibrium particle density of standard nuclear matter, ρ_o, to be calculated. This defines a nuclear matter radius constant r_o, a nuclear matter Fermi momentum P_o and a nuclear matter Fermi energy T_o, inter-related as follows:

$$\rho_o = \left(\frac{4}{3}\pi r_o^3\right)^{-1}, \tag{5}$$

$$P_o = \hbar\sqrt[3]{3\pi^2\rho_o/2}\,, \tag{6}$$

$$T_o = \frac{P_o^2}{2m} = \frac{\hbar^2}{2m}\left(\frac{9\pi}{8}\right)^{2/3}\frac{1}{r_o^2}\,, \tag{7}$$

where for m we have taken the average nucleon mass, equal to 938.926 MeV/c^2. Using ρ_o, P_o and T_o as convenient units we shall write

$$v_{12} = -2T_o\,\rho_o^{-1}\,f(r_{12}/a)\left\{\frac{1}{2}(1\mp\xi)\,\alpha \right.$$
$$\left. -\frac{1}{2}(1\mp\zeta)\left[\beta\,(p_{12}/P_o)^2 - \gamma\,(p_{12}/P_o)^{-1} + \sigma\,(2\overline{\rho}/\rho_o)^{2/3}\right]\right\}, \tag{8}$$

where α, β, γ, σ are now dimensionless parameters proportional to C_α, C_β, C_γ, C_σ, respectively.

We shall consider the function $f(r_{12}/a)$ to be normalized so that

$$\int d^3r_2\, f(r_{12}/a) = 1\ . \tag{9}$$

This makes the product $\rho_o^{-1} f(r_{12}/a)$ dimensionless. We shall eventually assume f to be a normalized Yukawa interaction

$$f(r/a) = \frac{1}{4\pi a^3}\frac{\mathrm{e}^{-r/a}}{r/a}\ , \tag{10}$$

but much of the development that follows is independent of this assumption.

The overall optimization and fine tuning of the seven parameters a, α, β, γ, σ, ξ and ζ by comparisons with a full range of diverse data is a problem for the future. The following preliminary set (explained in Section 9) will be used through most of this paper:

$$\begin{aligned} a &= 0.59542\ \text{fm}, \\ \alpha &= 3.60928, \quad \beta = 0.37597, \quad \gamma = 0.21329, \\ \sigma &= 1.33677, \quad \xi = 0.44003, \quad \zeta = 0.59778\,. \end{aligned} \tag{11}$$

These values correspond to the following nuclear properties:

$$
\begin{aligned}
&\text{radius constant of nuclear matter,} && r_o &&= 1.13 \text{ fm,} \\
&\text{Fermi energy of nuclear matter,} && T_o &&= 37.679 \text{ MeV,} \\
&\text{density of nuclear matter,} && \rho &&= 0.16545 \text{ fm}^{-3}, \\
&\text{volume energy coefficient,} && a_1 &&= 16.527 \text{ MeV,} \\
&\text{symmetry energy coefficient,} && J &&= 31.375 \text{ MeV,} \\
&\text{surface energy coefficient,} && a_2 &&= 20.268 \text{ MeV,} \\
&\text{curvature correction coefficient,} && a_3 &&= 10.996 \text{ MeV,} \\
&\text{compressibility coefficient,} && K &&= 301.27 \text{ MeV.}
\end{aligned}
\tag{12}
$$

3 The Thomas-Fermi Energy

In the Thomas-Fermi approximation the phase-space density of states for neutrons or protons is $(2/h^3)$,where h is Planck's constant. This makes the particle density in configuration space equal to $\rho = (4\pi/3)\, P^3\, (2/h^3)$, where P is the local Fermi momentum of the particles in question. When P equals P_o (the Fermi momentum of standard nuclear matter) the neutron and proton densities are $\rho_o/2$ each. We may thus write the neutron and proton density distributions in the form

$$\rho_n(\mathbf{r}) = (\rho_o/2)\, \Phi^3(\mathbf{r}), \qquad \rho_p(\mathbf{r}) = (\rho_o/2)\, \Psi^3(\mathbf{r}), \tag{13}$$

where

$$\Phi = P_n/P_o, \qquad \Psi = P_p/P_o, \tag{14}$$

with P_n, P_p the position-dependent local neutron and proton Fermi momenta.

The kinetic energy density of neutrons or protons with density ρ is $\frac{3}{5}\,(P^2/2m)\,\rho$, a quantity proportional to $\rho^{5/3}$. It follows that, after factoring out $\frac{1}{2}\rho_o T_o$ as the natural unit, the kinetic energy density associated with the neutron and proton distributions may be written as $\left(\frac{1}{2}\rho_o T_o\right)\, \frac{3}{5}\,(\Phi^5 + \Psi^5)$. The total ki-

netic energy, $K.E.$, is then the following integral over all space:

$$K.E. = \frac{1}{2}\rho_o T_o \int d^3r_1 \, \frac{3}{5}\left(\Phi_1^5 + \Psi_1^5\right) , \tag{15}$$

where Φ_1, Ψ_1 stand for the values of Φ, Ψ at the point $\mathbf{r}_1$.

The interaction energy, W, is an integral over all pairs of nucleons of the interaction energy v_{12}. It involves integrations over the relevant Fermi spheres at points 1 and 2, as well as over all spacial positions of these points. The momentum integrations are described in Appendix A, and the final result for the total energy, $E = K.E. + W$, may be written as an integral over all space of an energy density $\mathcal{E}(\mathbf{r}_1)$, viz:

$$E = \int d^3r_1 \, \mathcal{E}(\mathbf{r}_1) , \tag{16}$$

where

ERRORS.
See Part II
LBL 30395

$$\begin{aligned}
\mathcal{E}(\mathbf{r}_1) = {} & T_o(\rho_o/2)\frac{3}{5}\left(\Phi_1^5 + \Psi_1^5\right) \\
& - \frac{1}{2}T_o(\rho_o/2)\int d^3r_2 \, f\, \Phi_1^3\Phi_2^3 \left\{\alpha_\ell - \frac{6}{5}B_\ell\Phi_1^2 + \frac{3}{2}\gamma_\ell\, \Phi_>^{-1}\left[1 - \frac{1}{5}\frac{\Phi_<^2}{\Phi_>^2}\right]\right\} \\
& - \frac{1}{2}T_o(\rho_o/2)\int d^3r_2 \, f\, \Psi_1^3\Psi_2^3 \left\{\alpha_\ell - \frac{6}{5}B_\ell\Psi_1^2 + \frac{3}{2}\gamma_\ell\, \Psi_>^{-1}\left[1 - \frac{1}{5}\frac{\Psi_<^2}{\Psi_>^2}\right]\right\} \\
& - \; T_o(\rho_o/2)\int d^3r_2 \, f\, \Phi_1^3\Psi_2^3 \left\{\alpha_u - \frac{3}{5}B_u\left(\Phi_1^2 + \Psi_2^2\right) + \frac{3}{2}\gamma_u\, X_>^{-1}\left[1 - \frac{1}{5}\frac{X_<^2}{X_>^2}\right]\right\} \\
& + \frac{1}{2}e^2(\rho_o/2)^2 \int d^3r_2 \, \frac{\Psi_1^3\Psi_2^3}{r_{12}} \; .
\end{aligned} \tag{17}$$

In the above

$$
\begin{aligned}
\alpha_\ell &= \tfrac{1}{2}(1-\xi)\,\alpha = 1.01055, & \alpha_u &= \tfrac{1}{2}(1+\xi)\,\alpha = 2.59873,\\
\beta_\ell &= \tfrac{1}{2}(1-\zeta)\,\beta = 0.07561, & \beta_u &= \tfrac{1}{2}(1+\zeta)\,\beta = 0.30036,\\
\gamma_\ell &= \tfrac{1}{2}(1-\zeta)\,\gamma = 0.04289, & \gamma_u &= \tfrac{1}{2}(1+\zeta)\,\gamma = 0.17039,\\
\sigma_\ell &= \tfrac{1}{2}(1-\zeta)\,\sigma = 0.26884, & \sigma_u &= \tfrac{1}{2}(1+\zeta)\,\sigma = 1.06793,\\
B_\ell &= \beta_\ell + \tfrac{5}{6}\,\sigma_\ell = 0.29965, & B_u &= \beta_u + \tfrac{5}{6}\,\sigma_u = 1.19030.
\end{aligned}
\tag{18}
$$

The five lines in Eq.(17) are, in order, the kinetic energy density, and the neutron-neutron, proton-proton, neutron-proton and electrostatic interaction energy densities. (The proton charge density is $e\rho_p = e(\rho_o/2)\Psi^3$.) The notations Φ_1, Φ_2, Ψ_1, Ψ_2 refer to the values of Φ and Ψ at the points $\mathbf{r}_1$ and $\mathbf{r}_2$. The symbols $\Phi_>$, $\Phi_<$ stand for "the greater" or "the lesser" of Φ_1 and Φ_2, and similarly for $\Psi_>$, $\Psi_<$. The symbols $X_>$, $X_<$ stand for "the greater" or "the lesser" of Φ_1, and Ψ_2. The reason for making these distinctions is that different algebraic forms apply to the potential felt by a particle with a momentum less than or greater than the Fermi momentum characterizing the particles with which it is interacting (see Appendix A).

Eqs.(16,17) are the defining equations of our model, specifying the energy $E(\Phi,\Psi)$ as a functional of the relevant degrees of freedom, which are the functions $\Phi(\mathbf{r})$ and $\Psi(\mathbf{r})$ determining the neutron and proton densities. Note

that the parameters $\beta_{\ell,u}$ and $\sigma_{\ell,u}$ appear only in the combination $B_{\ell,u} = \beta_{\ell,u} + \frac{5}{6}\sigma_{\ell,u}$, so that *all the results following from Eq.(16), i.e. all energies and density distributions, depend on only six rather than seven parameters.*

In certain nuclear Thomas-Fermi studies attempts are sometimes made to improve the approximation to the kinetic energy density beyond the leading term proportional to $\rho^{5/3}$. This is often in the form of corrections associated with the gradient of the density or, more generally, in terms of power expansions in $\hbar$. Such corrections are not overwhelmingly important for most of the diffuse nuclear surface region—in a rough way of speaking they are less than some 10% down to a point in the surface where the density is about one-sixth of its bulk value [2,12,13]. The corrections do become qualitatively important at low densities, in particular in the quantal tail of the distributions. But by then a gradient expansion is not valid. Neither is a power expansion in $\hbar$ of a quantal tail governed by the non-analytic dependence on $\hbar$ typified by a wave function $\psi \sim \exp(-S/\hbar)$, where S is the action function. We believe that a physically well-founded and yet reasonably simple statistical treatment of the tail of nuclear and atomic density distributions is still a somewhat open problem.

Attempts to include corrections to the Thomas-Fermi kinetic energy are

often motivated by the wish to make the theory reproduce as accurately as possible, and without the readjustment of any parameters, a corresponding quantal, microscopic Hartree-Fock treatment. Our view of the role of a phenomenological Thomas-Fermi model with an adjustable effective interaction is somewhat different. Rather than regarding it as a (poor) approximation to a Hartree-Fock treatment, we consider it is a spectacular improvement of the Liquid Drop Model of average nuclear properties.

4 Standard Nuclear Matter ($\rho_n = \rho_p$)

When Φ and Ψ are constants independent of position, say $\Phi = \Psi = \Omega$, the integrals in Eq.(17) are trivial, and the following formula is readily found for the energy per particle, E/A, of standard nuclear matter (without Coulomb energy):

$$\eta \equiv \frac{E/A}{T_o} = \frac{3}{5}(1-\gamma)\,\Omega^2 - \frac{1}{2}\alpha\,\Omega^3 + \frac{3}{5}B\,\Omega^5\,. \tag{19}$$

It will be seen that the introduction of the new parameters γ and σ does not affect the functional form of Eq.(19), which remains the same as in the original Seyler-Blanchard model [2]! The coefficients of Ω^2 and Ω^5 merely change their values from 1 to $1-\gamma$ and from β to B, respectively.

The saturation requirement that $\eta(\Omega)$ should be a minimum for $\Omega = 1$, with value $\eta(1) \equiv \eta_o = -a_1/T_o$, leads to the equations:

$$\eta_o = \frac{3}{5}(1-\gamma) - \frac{1}{2}\alpha + \frac{3}{5}B\,, \tag{20}$$

$$0 = \frac{6}{5}(1-\gamma) - \frac{3}{2}\alpha + 3B\,. \tag{21}$$

The second derivative of $\eta(\Omega)$ evaluated at $\Omega = 1$ is the dimensionless compressibility coefficient κ, equal to K/T_o, where K is the conventional nuclear

compressibility coefficient. Thus

$$\kappa = \frac{6}{5}(1-\gamma) - 3\alpha + 12B\,. \tag{22}$$

Solving equations (20), (21), (22) for α, B, γ in terms of η_o and κ we find

$$\begin{aligned} \alpha &= 10\eta_o + \kappa \\ B &= \frac{5}{3}\eta_o + \frac{5}{18}\kappa \\ \gamma &= 1 - \frac{25}{3}\eta_o - \frac{5}{9}\kappa\,. \end{aligned} \tag{23}$$

These equations specify explicitly the interaction parameters α, B, γ needed to produce nuclear matter with the binding energy and compressibility described by η_o and κ. Note that through Eqs.(23) the compressibility coefficient K is related to γ by

$$K = \frac{9}{5}T_o + 15a_1 - \frac{9}{5}T_o\gamma = 315.73 - 67.828\gamma \ \text{ MeV}\,. \tag{24}$$

Thus, without the γ term, K has the unique value 315.73 MeV (with our choice of interaction parameters). More generally, κ is a (decreasing) linear function of γ only. It does not depend on the other parameters of the interaction, in particular not on the density-dependence parameter σ. For the value of γ used in this paper, K is equal to 301.27 MeV.

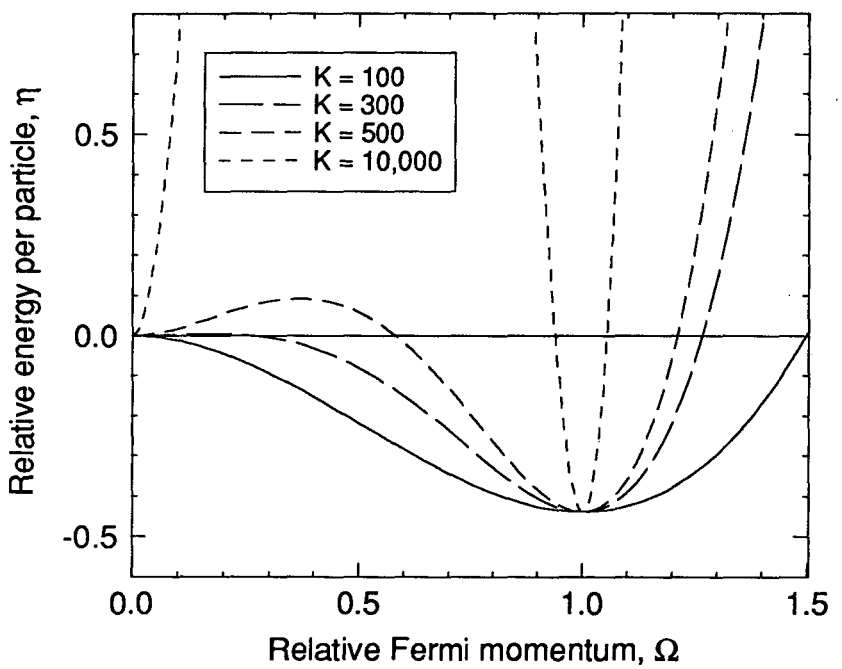

Fig. 1 The binding energy per particle of standard nuclear matter (in units of T_o) as a function of Ω, the Fermi momentum in units of P_o. (The relative density ρ/ρ_o is equal to Ω^3.) The compressibility $K = 300$ MeV is approximately the value we have deduced from experiment. The value $K = 10,000$ illustrates the approach of our model to the limiting case of an incompressible liquid drop.

Fig. 1 shows the appearance of $\eta(\Omega)$ for different values of γ or, equivalently, of K. By making γ tend to minus infinity (i.e., $K \to \infty$) one obtains the incompressible liquid drop, which is thus automatically included in our model as a limiting case. Conversely, by increasing γ to the limiting value $(1 - \frac{25}{3}\eta_o) = 4.6552$, one arrives at the (unphysical) situation where K has vanished, and the minimum at $\Omega = 1$ has become a point of inflection. This is associated with the fact that $\frac{3}{5}B$, the coefficient of the Ω^5 term in Eq.(19), has become negative, and this causes a collapse of the system to infinite density with infinite binding. For intermediate values of γ, such that $1 - 5\eta_o < \gamma < 1 - \frac{25}{3}\eta_o$ (i.e. $3.1932 < \gamma < 4.6552$) nuclear matter in our model is metastable, separated from the collapsed configuration at infinite density, by an energy barrier of finite height. At $\gamma = 1 - 5\eta_o$ the barrier becomes infinite and for $\gamma < 1 - 5\eta_o$ nuclear matter at $\Omega = 1$ is the absolute minimum. Very large values of γ are presumably unphysical, but intermediate values might be useful for parameterizing situations where the equation of state becomes relatively soft at high densities.

5 Uniform Nuclear Matter ($\rho_n \neq \rho_z$)

In the case $\Phi \neq \Psi$ the energy per particle of uniform nuclear matter is given by:

$$\begin{aligned}\eta = \Bigg\{ & \frac{3}{5}\left(\Phi^5 + \Psi^5\right) - \frac{1}{2}\Phi^6\left(\alpha_\ell - \frac{6}{5}B_\ell\Phi^2 + \frac{6}{5}\gamma_\ell\Phi^{-1}\right) \\ & - \frac{1}{2}\Psi^6\left(\alpha_\ell - \frac{6}{5}B_\ell\Psi^2 + \frac{6}{5}\gamma_\ell\Psi^{-1}\right) \\ & - \Phi^3\Psi^3\left[\alpha_u - \frac{3}{5}B_u\left(\Phi^2 + \Psi^2\right) + \frac{3}{2}\gamma_u X_>^{-1}\left(1 - \frac{1}{5}\frac{X_<^2}{X_>^2}\right)\right]\Bigg\} \Big/ \left(\Phi^3 + \Psi^3\right),\end{aligned} \tag{25}$$

where $X_>$, $X_<$ stand for "the greater" or "the lesser" of Φ, Ψ.

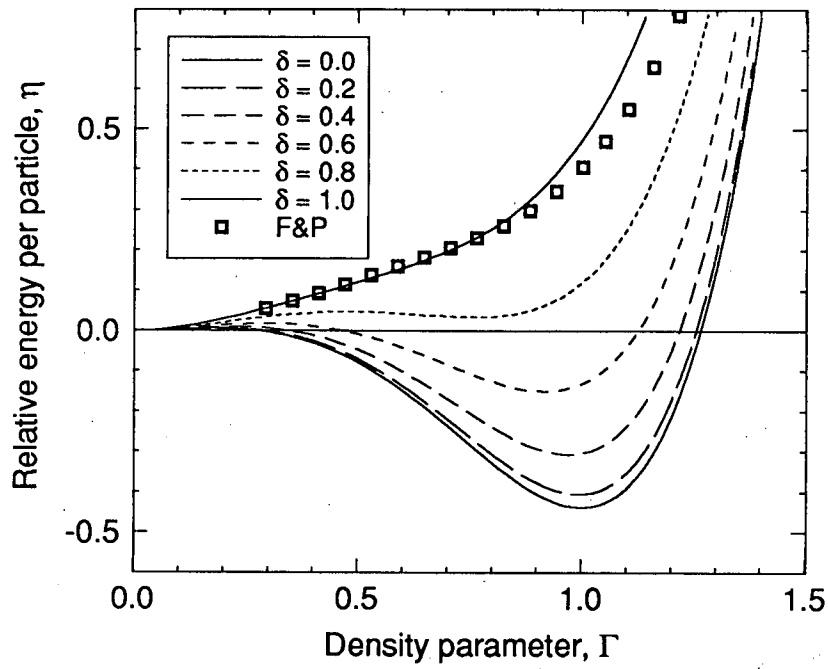

Fig. 2 The energy per particle of uniform nuclear matter (in units of T_o) for different values of the relative neutron excess $\delta = (\rho_n - \rho_p)/(\rho_n + \rho_p)$. The parameter Γ is related to the relative density by $\Gamma^3 \equiv \rho/\rho_o$. Neutron matter corresponds to $\delta = 1$ and is given by the upper solid curve. Neutron matter at a density equal to the neutron density prevailing in equilibrium standard nuclear matter (i.e. $\rho_n = \rho_o/2$) corresponds to $\Gamma = (1/2)^{1/3} \doteq 0.7937$. Up to such a density the solid curve agrees closely with the theoretical estimate of Ref.[14], given by the squares.

Fig. 2 illustrates the appearance of $\eta(\Phi, \Psi)$ for various values of the relative neutron excess δ, defined by

$$\delta = \frac{\Phi^3 - \Psi^3}{\Phi^3 + \Psi^3} \,. \tag{26}$$

Neutron matter corresponds to $\delta = 1$. Our interaction parameters were chosen so that for this limiting case the binding energy curve would agree approximately with the calculations of Ref.[14]. Figure 3 shows how, in our model, properties of neutron matter may be varied while keeping the binding properties of familiar nuclei essentially unchanged (by demanding that the nuclear symmetry energy coefficient remain fixed). In fact, by increasing the relative strength of the binding force between like particles, one could make neutron matter metastable with respect to density changes (i.e. to exhibit a minimum in Fig. 3), or even absolutely stable (i.e. bringing the minimum below the abscissa). One does not expect this to correspond to physical reality, but our model is flexible enough to describe situations approaching to a varying degree such a hypothetical case. Equation (25) may be used to derive closed expressions for the compressibility of nuclear matter with an arbitrary value of the neutron excess, a subject we hope to treat in a future publication. (For a study of this problem see Ref.[15].)

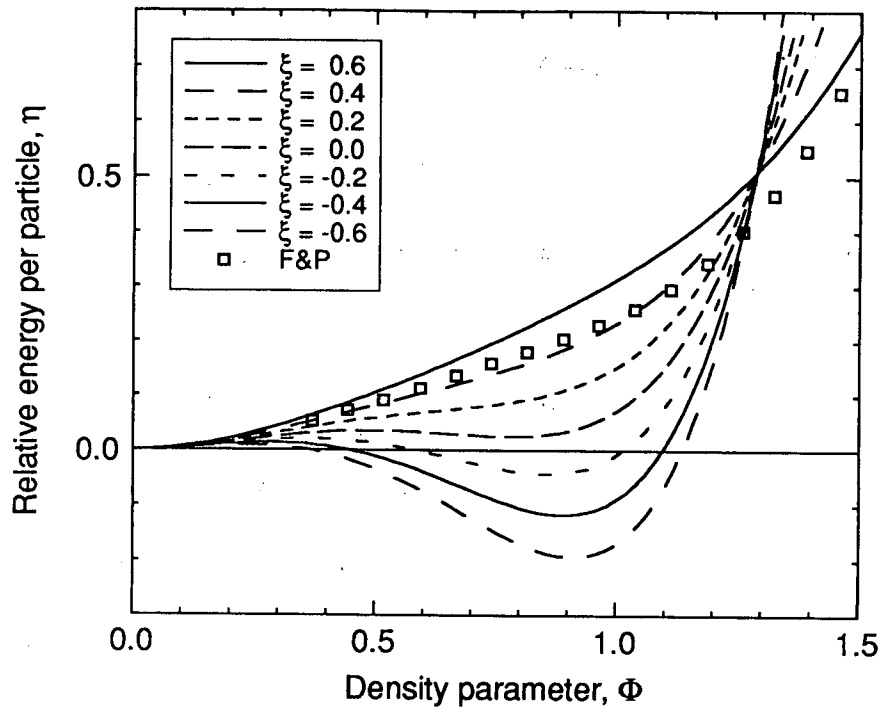

Fig. 3 The energy per particle of neutron matter (in units of T_o), for various values of the parameter ξ, which is a measure of the relative strength of interactions between like and unlike particles. The cube of the parameter Φ is the neutron matter density in units of $\rho_o/2$. For each value of ξ the other interaction parameters were readjusted so as to keep the binding, density and symmetry energy coefficient of standard nuclear matter fixed. For a value of ξ equal to about 0.44 the Thomas-Fermi calculation agrees closely (up to $\Phi \approx 1$) with the estimates of Ref.[14], given by the squares. For ξ less than about 0.2, the energy plot develops a metastable minimum, which becomes stable for ξ less than about -0.1.

6 The Euler Equations

By demanding that the total energy, Eqs.(16,17), be stationary with respect to arbitrary infinitesimal particle-conserving variations $\delta\rho_n$, $\delta\rho_p$ (or, equivalently, $\delta\Phi$, $\delta\Psi$) we obtain the Euler equations defining the equilibrium distributions of the neutron and proton densities. Recalling that $\delta\rho_n = (\rho_o/2)3\Phi^2\,\delta\Phi$ and $\delta\rho_p = (\rho_o/2)3\Psi^2\,\delta\Psi$, and denoting by $\delta_n E$ and $\delta_p E$ the associated energy changes, we thus have to satisfy the following conditions:

$$\begin{aligned} \delta_n E &= T_o \int d^3r_1\, \Phi_1^2 \delta\rho_n(1) + \delta_n W = 0\,, \\ \delta_p E &= T_o \int d^3r_1\, \Psi_1^2 \delta\rho_p(1) + \delta_p W = 0\,. \end{aligned} \tag{27}$$

Instead of grinding through the algebra of taking the variations of W in Eq.(27), we make use of a short-cut based on the definitions of the neutron and proton potentials, U_n and U_p, in terms of the variations $\delta_n W$ and $\delta_p W$, viz. :

$$\begin{aligned} \delta_n W &= \int d^3r_1\, U_n(1)\delta\rho_n(1), \\ \delta_p W &= \int d^3r_1\, U_p(1)\delta\rho_p(1), \end{aligned} \tag{28}$$

where explicit expressions for U_n and U_p have been derived in Appendix A, Eqs.(78) and (79), as an intermediate step in evaluating the interaction

energy W. If the Eqs.(27) are to be satisfied for arbitrary particle preserving variations, the integrands in those equations must be constants, (equal to the chemical potentials of the neutrons and protons).

Hence,

$$\Lambda_n = \Phi_1^2 \; - \; \int d^3r_2\, f\, \Phi_2^3 \left\{ \alpha_\ell - B_\ell \left(\frac{3}{5}\Phi_2^2 + \Phi_1^2 \right) + \gamma_\ell \left\langle \begin{array}{l} \Phi_1^{-1} \\ \Phi_2^{-1} \left[\frac{3}{2} - \frac{1}{2}(\Phi_1/\Phi_2)^2 \right] \end{array} \right. \right\}$$

$$- \; \int d^3r_2\, f\, \Psi_2^3 \left\{ \alpha_u - B_u \left(\frac{3}{5}\Psi_2^2 + \Phi_1^2 \right) + \gamma_u \left\langle \begin{array}{l} \Phi_1^{-1} \\ \Psi_2^{-1} \left[\frac{3}{2} - \frac{1}{2}(\Phi_1/\Psi_2)^2 \right] \end{array} \right. \right\}$$

and

$$\Lambda_p = \Psi_1^2 \; - \; \int d^3r_2\, f\, \Psi_2^3 \left\{ \alpha_\ell - B_\ell \left(\frac{3}{5}\Psi_2^2 + \Psi_1^2 \right) + \gamma_\ell \left\langle \begin{array}{l} \Psi_1^{-1} \\ \Psi_2^{-1} \left[\frac{3}{2} - \frac{1}{2}(\Psi_1/\Psi_2)^2 \right] \end{array} \right. \right\}$$

$$- \; \int d^3r_2\, f\, \Phi_2^3 \left\{ \alpha_u - B_u \left(\frac{3}{5}\Phi_2^2 + \Psi_1^2 \right) + \gamma_u \left\langle \begin{array}{l} \Psi_1^{-1} \\ \Phi_2^{-1} \left[\frac{3}{2} - \frac{1}{2}(\Psi_1/\Phi_2)^2 \right] \end{array} \right. \right\}$$

$$+ \; e^2(\rho_o/2T_o) \int d^3r_2\, \Psi_2^3/r_{12} \; . \tag{29}$$

In the above equations Λ_n, Λ_p are the chemical potentials of the neutrons and protons in units of T_o. In the terms multiplying γ the upper line is to be used if the symbol with suffix 1 is greater than the symbol with suffix 2, otherwise the lower line. Eqs.(29) are cubic expressions in Φ_1 and Ψ_1, and

may be written in the form:

$$\Phi_1^3 - C_1^n \Phi_1 - C_0^n = 0\,, \quad \Psi_1^3 - C_1^p \Psi_1 - C_0^p = 0\,, \tag{30}$$

where

$$C_1^{n,p} = B_{n,p}/A_{n,p}\,, \quad C_0^{n,p} = C_{n,p}/A_{n,p}\,, \tag{31}$$

with

$$\begin{aligned}
A_n &= 1 + \int d^3r_2\, f\, \left[B_\ell \Phi_2^3 + \frac{1}{2}\gamma_\ell \Theta\left(\Phi_2 - \Phi_1\right) + B_u \Psi_2^3 + \frac{1}{2}\gamma_\ell \Theta\left(\Psi_2 - \Phi_1\right)\right], \\
B_n &= \Lambda_n + \int d^3r_2\, f\, \left[\alpha_\ell \Phi_2^3 - \frac{3}{5}B_\ell \Phi_2^5 + \frac{3}{2}\gamma_\ell \Phi_2^2\, \Theta\left(\Phi_2 - \Phi_1\right)\right. \\
&\qquad\qquad \left. + \alpha_u \Psi_2^3 - \frac{3}{5}B_u \Psi_2^5 + \frac{3}{2}\gamma_u \Psi_2^2\, \Theta\left(\Psi_2 - \Phi_1\right)\right], \\
C_n &= \int d^3r_2\, f\, \left[\gamma_\ell \Phi_2^3 \Theta\left(\Phi_1 - \Phi_2\right) + \gamma_u \Psi_2^3 \Theta\left(\Phi_1 - \Psi_2\right)\right], \\
A_p &= 1 + \int d^3r_2\, f\, \left[B_\ell \Psi_2^3 + \frac{1}{2}\gamma_\ell \Theta\left(\Psi_2 - \Psi_1\right) + B_u \Phi_2^3 + \frac{1}{2}\gamma_\ell \Theta\left(\Phi_2 - \Psi_1\right)\right], \\
B_p &= \Lambda_z + \int d^3r_2\, f\, \left[\alpha_\ell \Psi_2^3 - \frac{3}{5}B_\ell \Psi_2^5 + \frac{3}{2}\gamma_\ell \Psi_2^2\, \Theta\left(\Psi_2 - \Psi_1\right)\right. \\
&\quad \left. + \alpha_u \Phi_2^3 - \frac{3}{5}B_u \Phi_2^5 + \frac{3}{2}\gamma_u \Phi_2^2\, \Theta\left(\Phi_2 - \Psi_1\right)\right] - (\mathrm{e}^2 \rho_o/2T_o) \int d^3r_2\, \Psi_2^3/r_{12}\,, \\
C_p &= \int d^3r_2\, f\, \left[\gamma_\ell \Psi_2^3 \Theta\left(\Psi_1 - \Psi_2\right) + \gamma_u \Phi_2^3 \Theta\left(\Psi_1 - \Phi_2\right)\right]\,.
\end{aligned} \tag{32}$$

In the above, $\Theta(x)$ is the step function $\Theta(x) = 1$ for $x > 0$, $\Theta(x) = 0$ for $x < 0$. (This is an alternative way of writing the non-analytic γ-terms.) The Euler equations may be used to determine $\Phi(\mathbf{r})$ and $\Psi(\mathbf{r})$ by numerical

iteration. (See Appendix B.) Fig. 4 shows, as an example, calculated (and measured) density distributions for three nuclei. This comparison suggests that a better fit could have been obtained by an increase in the calculated surface diffuseness. This can be achieved by reducing the compressibility coefficient K below 301.27 MeV, which means an increase of the coefficient γ over its illustrative value of 0.21329. (See next section.)

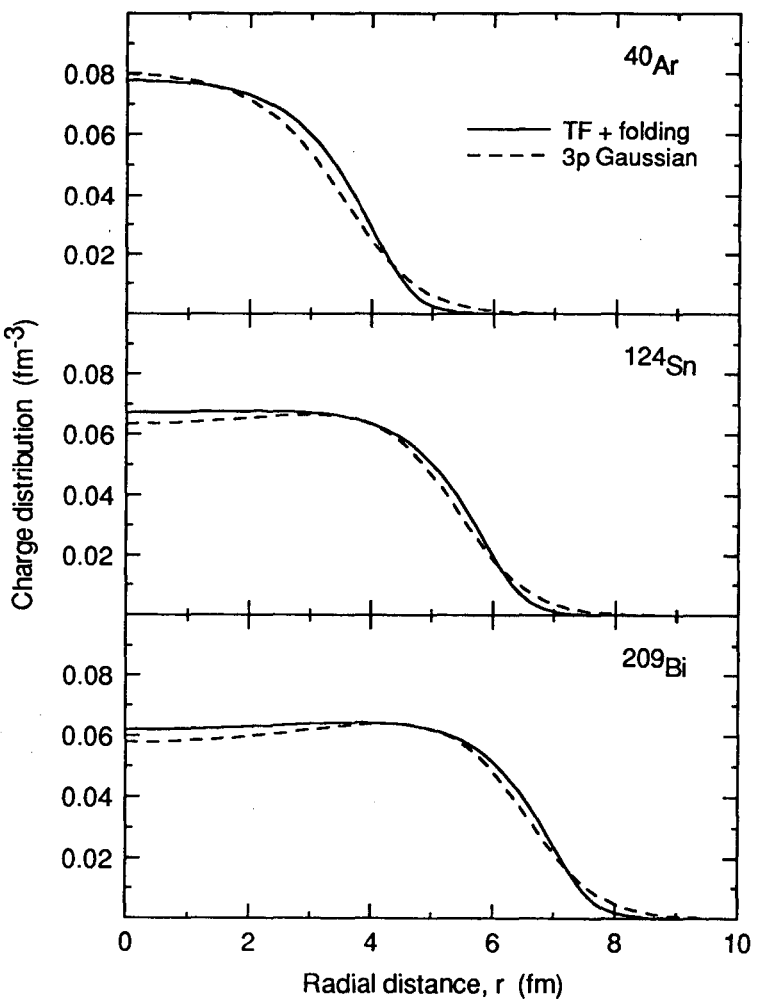

Fig. 4 The calculated Thomas-Fermi charge distribution of three nuclei (after folding in the proton size) are compared with experimental distributions represented by a so-called 3-parameter Gaussian fit. The RMS radii of the calculated and measured distributions are about equal. A better fit could have been obtained by increasing the calculated surface diffuseness (resulting in a reduction of the compressibility coefficient).

7 Semi-Infinite Distributions

In order to study the surface properties of nuclear matter, the Euler equations above may be adapted for treating semi-infinite distributions bounded by a plane surface. This is achieved by the simple replacement [2]:

$$\int d^3r_2\, f \Longrightarrow \int_{-\infty}^{\infty} dx_2\, g\,, \tag{33}$$

where x is a coordinate along the inward normal to the surface and

$$g = \frac{1}{2a} \exp(-|x_1 - x_2|/a)\,. \tag{34}$$

The solid curve in Fig. 5 shows the surface profile in the case of standard, semi-infinite matter, resulting from solving the modified Euler equations. The dashed curve is the result of folding into this profile a Yukawa nucleon form factor with an RMS size of 0.85 fm, corresponding to the measured proton charge distribution [16].

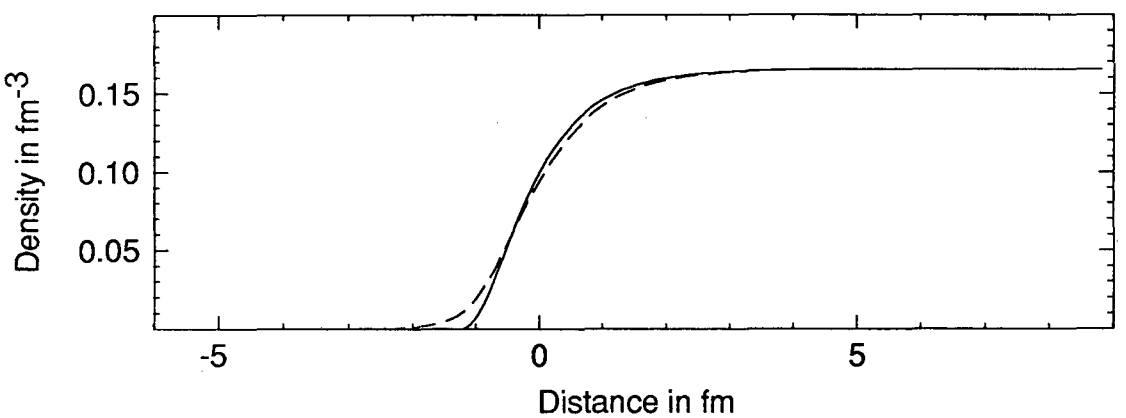

Fig. 5 The calculated Thomas-Fermi density profile of standard, semi-infinite nuclear matter is shown by the solid curve. The dashed line is the result of folding in a Yukawa nucleon form factor with an RMS size of 0.85 fm, corresponding to the measured charge distribution of a proton. The distance along the abscissa is measured from the location of the effective sharp surface.

The surface energy per unit area, s, is given by the following integral along the normal to the surface [2]:

$$s = \mathcal{E}_\infty \int_{-\infty}^{\infty} dx \left(\frac{\mathcal{E}}{\mathcal{E}_\infty} - \frac{\rho}{\rho_\infty} \right) , \tag{35}$$

where $\mathcal{E}$ is the energy density function obtained from Eq.(17) by making the replacements given by Eqs.(33,34), and by omitting the Coulomb energy. The quantities ρ_∞ and $\mathcal{E}_\infty$ are, respectively, the asymptotic density and energy density values that hold in the interior, far from the surface. The surface energy coefficient a_2 is related to s by $a_2 = 4\pi r_o^2 s$. With the binding energy and density of nuclear matter held fixed, a_2 in our model depends only on the range a of the Yukawa interaction and on the parameter γ. Since γ is in a one to one relationship with the compressibility K, one may plot a_2 as a function of K for a fixed range a or, preferably, for a fixed surface width b. A very interesting property of such plots is illustrated in Fig. 6. We see that if the surface width (diffuseness) is fixed, the relation between a_2 and K is linear to an astonishing degree, even though the linearity is not algebraically exact. Furthermore, to the extent that b and a_2 are quite well determined experimentally, our model provides a way of translating the measurements of b and a_2 into a fairly reliable estimate of K. If the value $b \approx 1$ fm is

taken as representative for the surface diffuseness and $a_2 \approx 20$ MeV for the surface energy coefficient, the compressibility predicted on the basis of Fig. 6 is about 300 MeV. If, following the comparison in Fig. 4, the slightly larger value $b \approx 1.1$ fm were adopted, K would be reduced to about 250 MeV. On the other hand, a recent comparison of the measured giant monopole resonance energies with the predictions of the present Thomas-Fermi model [10] shows good agreement when the baseline value $K = 301.27$ MeV is used. A more definitive prediction of K will have to await the simultaneous optimization of the model parameters using all relevant data. These will include, in particular, the heights of the nuclear fission barriers, a problem that we shall report on in a future publication.

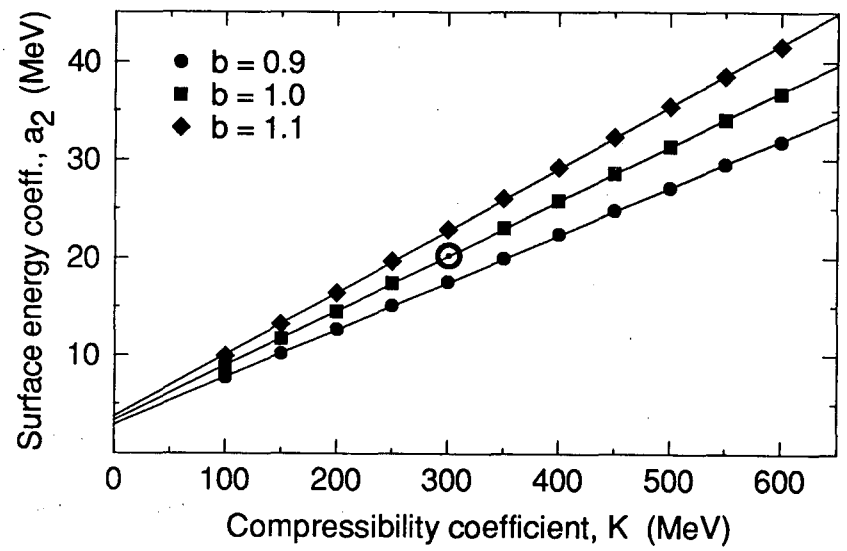

Fig. 6 Each set of symbols represents the result of calculating the surface energy of semi-infinite nuclear matter using interaction parameters chosen so as to give the same volume energy per particle, the same equilibrium density and the same surface width b, but different compressibility coefficients K. The value of b deduced from measured charge distributions ($b \approx 1$ fm), together with the value of a_2 deduced from fits to measured binding energies ($a_2 \approx 20$ MeV), leads to an estimated value for K of about 300 MeV. (Some evidence for a value of b greater than 1 fm is suggested by Fig.4.) Note the astonishingly linear appearance of the graph resulting from plotting a_2 vs. K at fixed b. (The lines are straight line fits to the calculated points.)

8 Optical Model Potentials

The potential $U_n(r_1, p)$ felt by a neutron traversing a region of space where the neutron and proton densities are specified by $\Phi(r)$ and $\Psi(r)$ is given by Eq.(76) in Appendix A. It is a function of position and of the neutron's momentum p at the point in question. The corresponding expression for the proton potential $U_p(r_1, p)$ is Eq.(77). A comparison of the potential wells represented by Eqs.(76,77) with experimental data on nucleon-nucleus scattering would require the solution of the scattering problem in the above momentum dependent potentials. In the absence of such an analysis we can make some progress by comparing the central depths of optical-model potentials fitted to scattering data with the depths predicted by our model for uniform nuclear matter. But it should be borne in mind that such a comparison is not unambiguous, since the optical-model fits are made, at each bombarding energy, with a static, momentum-independent potential, rather than with a potential of the form of Eqs.(76,77).

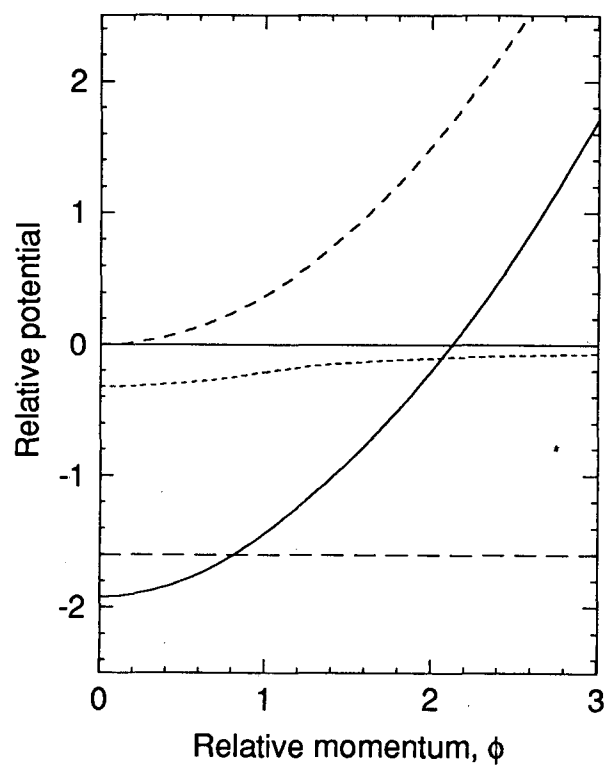

Fig. 7 The calculated momentum dependence of the potential felt by a neutron traveling through standard nuclear matter. (The potential is in units of T_o and the momentum is in units of P_o). The total potential (solid curve) is made up of a negative constant (long dashes), plus the parabolic term $\beta\phi^2$ (medium dashes) and the γ-term proportional to ϕ^2 for $\gamma < 1$, and to ϕ^{-1} for $\gamma > 1$ (short dashes).

Let us consider then the case of a neutron with momentum $p = \phi P_o$ traveling through standard uniform nuclear matter, specified by $\Phi = \Psi = 1$. Using the notation $u = U/T_o$, we find for the neutron potential u the simple expression (illustrated in Fig. 7):

$$u(\phi) = -\alpha + \frac{3}{5}\beta + \frac{4}{3}\sigma + \beta\phi^2 - \gamma \begin{cases} \phi^{-1} & \text{for } \phi > 1 \\ \frac{3}{2} - \frac{1}{2}\phi^2 & \text{for } \phi < 1 \,. \end{cases} \tag{36}$$

For momenta $p < P_o$ (i.e. $\phi < 1$) we may write the result as:

$$u_< = -\frac{9 - 21\eta_o - 5\sigma}{9 - 15\eta_o - 5\sigma} + \frac{3 - 15\eta_o - 5\sigma}{9 - 15\eta_o - 5\sigma}\varepsilon, \tag{37}$$

where ε, equal to $u + \phi^2$, is the neutron's total energy (kinetic plus potential) in units of T_o. (We have used Eqs.(23) to eliminate α and β in favor of η_o and σ.) Eq.(37) states that, for $p < P_o$, the potential $u_<$ is independent of γ, the only parameter in Eq.(37) being the density-dependence coefficient σ. (The value of η_o is essentially fixed by measured nuclear binding energies and sizes.) Moreover, the potential is strictly linear in the energy ε and may be further re-written as

$$u_< - (\eta_o - 1) = \frac{5 - 15\eta_o - 5\sigma}{9 - 15\eta_o - 5\sigma}(\varepsilon - \eta_o). \tag{38}$$

In a plot of $u_<$ vs. ε this is a straight line with slope $(3 - 15\eta_o - 5\sigma)/(9 - 15\eta_o - 5\sigma)$, pivoted at the point $u_< = \eta_o - 1$, $\varepsilon = \eta_o$, (i.e. $U_< = -54.206$ MeV,

$E = -16.527$ MeV) independently of the value of σ. This fixed pivoting point will be recognized as the depth of the potential experienced by a particle with binding energy η_o, i.e. a particle at the top of the Fermi sphere. On the other hand, the potential felt by a particle with zero kinetic energy (at the bottom of the potential well) is obtained by setting $\varepsilon - u_< = 0$, which gives

$$u_<(\phi = 0) = -\frac{3}{2} + \frac{7}{2}\eta_o + \frac{5}{6}\sigma \tag{39}$$

i.e.

$$U_<(0) = -72.39 \text{ MeV} \tag{40}$$

For the potential $u_>$ felt by a particle with $p > P_o$ ($\phi > 1$) we find

$$\begin{aligned} u_> &= \left(-\alpha + \frac{3}{5}\beta + \frac{4}{3}\sigma\right) + \beta\phi^2 - \gamma\phi^{-1} \\ &= \left(-\frac{3}{2} + \frac{7}{2}\eta_o + \frac{3}{2}\gamma + \frac{5}{6}\sigma\right) + \left(\frac{1}{2} - \frac{5}{2}\eta_o - \frac{1}{2}\gamma - \frac{5}{6}\sigma\right)(\varepsilon - u_>) \\ &\quad - \gamma(\varepsilon - u_>)^{-1/2}. \end{aligned} \tag{41}$$

For $\gamma = 0$ this reduces to the same straight line as Eq.(37). In that case, the energy ε_o at which the potential would turn repulsive is given by setting $u_> = 0$ in Eq.(37), which leads to

$$\varepsilon_o = \frac{9 - 21\eta_o - 5\sigma}{3 - 15\eta_o - 5\sigma}. \tag{42}$$

Without the density-dependent term in the effective interaction ($\sigma = 0$) this would give $\varepsilon_o = 1.9011$ i.e. an energy of 71.63 MeV.

An explicit solution of Eq.(41) for $u_>$ as a function of ε involves the solution of a cubic, but a parametric plot of $u_>$ vs. ε is even more elementary: pick a value of $\varepsilon - u_>$ (equal to τ, say, the neutron's dimensionless kinetic energy), calculate $u_>$ from Eq.(41) and then calculate ε from $\varepsilon = u_> + \tau$. Fig. 8 shows a comparison of Eq.(41) with a summary of optical model potential depths taken from Ref.[17]. It is clear that for $\gamma = 0$ a fit to the potential depths would be impossible using $\sigma = 0$. (The potential would turn repulsive at an incident energy of about 72 MeV.) With σ included, an approximate fit can be obtained even without the γ term. Including a small value of γ, as suggested by evidence from nuclear surface properties (see Section 7) makes possible a fair representation of the energy dependence of the optical model potential depths in the range of energies from -70 MeV. to about 200 MeV.

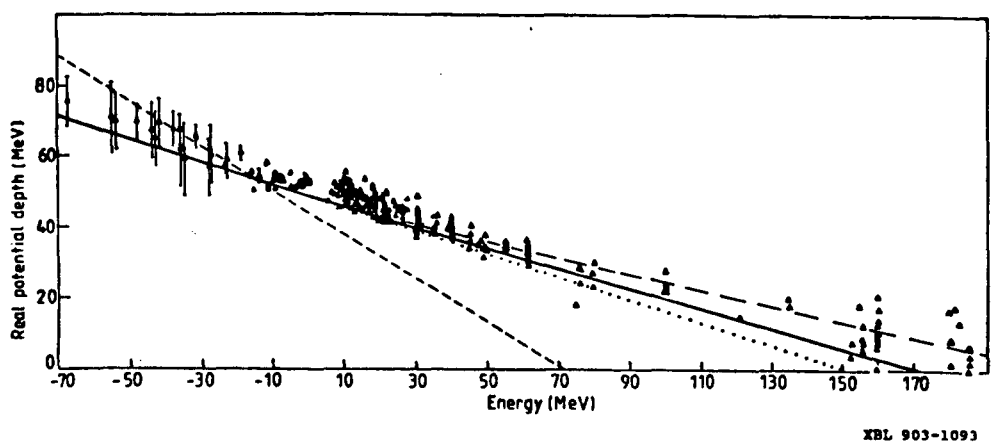

Fig. 8 A compilation of the measurements of the depth of the optical model potential taken from Ref.[17] is compared with the Thomas-Fermi calculations. The short-dashed line would be the result of using the original Seyler-Blanchard model [8] with $\gamma = 0$ and $\sigma = 0$. Increasing σ to 1.33677 gives the dotted line (and the same compressibility). Taking γ to have the value which reproduces approximately the measured surface diffuseness ($\gamma = 0.21329$) bends the curve up away from the abscissa to give the solid curve. (The compressibility is now $K = 301.27$ MeV.) All the curves pass through the fixed point at $U = -54.206$ MeV, $E = -16.527$ MeV and are strictly linear and independent of γ for $E < -16.527$ MeV. The long-dashed line results from increasing the value of γ to 0.45305, which corresponds to $K = 285$ MeV.

It is worth stressing the simplicity of the dependence of u on the parameters of our model. Thus, the overall scale of the potential depth is proportional to the energy unit T_o, which scales inversely with the square of the radius constant r_o (known to within a percent or so). The overall slope of the plot of U vs. energy is governed by the parameter σ. The plot is strictly linear for energies below the Fermi energy. For energies above the Fermi energy the plot would continue to be linear if γ were zero. A finite value of γ introduces a bending of the plot, away from the abscissa for $\gamma > 0$, towards it for $\gamma < 0$. According to Fig. 8 there is thus some evidence from the optical potential depths for a small positive value of γ, confirming the independent evidence from the nuclear surface properties. Both sets of data thus suggest a compressibility coefficient somewhat smaller than the baseline value of 315.73 MeV resulting from taking $\gamma = 0$ in Eq.(24).

In the case of uniform nuclear matter with $\rho_n \neq \rho_p$, the neutron and proton potentials are found from Eqs.(76,77) by replacing $\int d^3r_2\, f$ by unity. In particular, for a neutron or proton at the top of its respective Fermi sphere, the potentials are obtained by putting $\phi = \Phi$, $\psi = \Psi$. The difference between

these potentials (in the case that $\rho_n > \rho_p$) is then given by,

$$\begin{aligned} u_n - u_p &= -\alpha_\ell(\Phi^3 - \Psi^3) + \frac{8}{5}B_\ell(\Phi^5 - \Psi^5) - \gamma_\ell(\Phi^2 - \Psi^2) \\ &- \alpha_u(\Psi^3 - \Phi^3) + \frac{3}{5}B_u(\Psi^5 - \Phi^5) + B_u(\Psi^3\Phi^2 - \Phi^3\Psi^2) \\ &- \gamma_u\left(\Psi^3\Phi^{-1} - \frac{3}{2}\Phi^2 + \frac{1}{2}\Psi^2\right). \end{aligned} \tag{43}$$

Writing $(\Phi^3 - \Psi^3)/(\Phi^3 + \Psi^3) = \delta$ and expanding to first order in δ we find:

$$u_n - u_p = \left(-2\alpha_\ell + 2\alpha_u + \frac{16}{3}B_\ell - \frac{8}{3}B_u - \frac{4}{3}\gamma_\ell + \frac{8}{3}\gamma_u\right)\delta\,. \tag{44}$$

Using the expression for the dimensionless symmetry energy coefficient ω_1, given by J/T_o, (Appendix C, Eq.(92)) we find

$$\frac{u_n - u_p}{\delta} = 4\omega_1 - \frac{4}{3}\,, \tag{45}$$

or

$$\frac{U_n - U_p}{\delta} = \frac{\partial(U_n - U_p)}{\partial\delta} = 4J - \frac{4}{3}T_o\,. \tag{46}$$

By recalling the definition

$$J = \frac{1}{2}\frac{\partial^2(E/A)}{\partial\delta^2} \tag{47}$$

and using

$$\frac{\partial(U_n - U_z)}{\partial\delta} = 2\frac{\partial U_n}{\partial\delta} \tag{48}$$

we find,

$$\frac{\partial U_n}{\partial \delta} = \frac{\partial^2 (E/A)}{\partial \delta} - \frac{2}{3} T_o \,. \tag{49}$$

Since $\frac{2}{3}T_o$ is readily verified to be the second derivative of the kinetic energy per particle with respect to δ, we may write:

$$\frac{\partial U_n}{\partial \delta} = \frac{\partial^2 (W/A)}{\partial \delta^2} \,, \tag{50}$$

where W/A is the interaction energy per particle. Hence the theorem: "The first derivative with respect to the relative neutron excess of the potential felt by a neutron at the top of its Fermi sphere, and the second derivative of the interaction energy per particle with respect to the same variable, are equal."

The above equations enable one to predict the isospin dependence of the optical potential (for particles of the top of the Fermi sphere) in terms of the known symmetry energy coefficient. For example, using Eq.(46), one estimates that the difference in the depths of the neutron and proton potentials in ^{208}Pb should be about 75.3δ or 11 MeV if δ is taken to be about 0.15, Ref.[18]. According to Ref.[19], p.239, the measured difference is about 14 MeV. Thus we are assured that our model reproduces, at least approximately, not only the energy dependence of the optical potential but also its isospin

dependence.

9 Determination of a Preliminary Set of Interaction Parameters

A fast computer program was developed to calculate the Thomas-Fermi masses of spherically symmetric nuclei. These masses were compared with "corrected" measured masses of a sample of 336 isotopes of 20 elements with atomic numbers between Z=8 and Z=100. The measured masses were corrected for shell effects (including deformations, Ref.[20]), even-odd mass differences and the Wigner or "congruence" energy. Our interpretation of the latter (called the "Matching Energy" in Ref.[3]) is in terms of a relatively stronger interaction energy between pairs of nucleons in essentially congruent quantized orbits (i.e. orbits with essentially identical spatial density distributions $|\psi|^2$, whose nodes and antinodes are everywhere matched). In addition to an even-odd term, this congruence leads to an extra binding whose estimated functional dependence on N and Z is of the form,

$$E_{CON} \approx -a_o + W(|I| + \Delta)\,, \tag{51}$$

where $\Delta = A^{-1}$ for odd-odd nuclei with $N = Z$, and zero otherwise. The parameter W is known from previous studies to be about 30 MeV, and was

fixed at that value. The parameter a_o was considered as adjustable. (The congruence energy, like the even-odd correction, is absent in a statistical, continuum treatment of the Thomas-Fermi type, and must be allowed for by an additional semi-empirical term.)

A fit to the corrected experimental masses (characterized by an rms deviation of 1.05 MeV) was obtained [20] by varying the six interaction parameters a, α, B, γ, ξ, ζ, as well as a_o (which turned out to have the value -19.267 MeV). The fit was constrained by the demand that the density distributions for the protons should roughly reproduce measurements, and that the neutron-matter binding energy curve in the region of moderate densities should be close to the estimate in Ref.[14], as illustrated in Fig. 2. The charge distribution constraint was expressed by the condition that the nuclear matter radius constant should be 1.13 fm and that the (Süssmann) width b [21] of the charge distribution should be 1 fm after folding-in a proton charge form factor with an RMS size $\langle r^2 \rangle^{1/2} = 0.85$ fm [16]. Because of the additivity of the Süssmann widths under the folding operation, we may write,

$$b_{TF}^2 + b_{proton}^2 = 1 \text{ fm}^2 , \tag{52}$$

where b_{TF} is the width of the Thomas-Fermi surface before folding, and b_{proton}

is related to $\langle r^2 \rangle$ by

$$b^2_{proton} = \langle r^2 \rangle / 3 \,. \tag{53}$$

Hence the condition on the Thomas-Fermi density distributions is that b_{TF} should be equal to $\sqrt{1 - b^2_{proton}} = 0.871$ fm. No systematic attempt was made to optimize the fit to experimental charge distributions, such as those shown in Fig. 4, which thus remains quite rough at this stage. The optimization of all the model parameters awaits the inclusion in the discussion of fission barrier heights, a problem that we will consider in a future publication.

The parameter σ, which shows up only in the energy dependence of the optical potential, and is thus conveniently decoupled from the other parameters, was determined by demanding approximate agreement with the trend of the data in Fig. 8.

10 The Truncated Thomas-Fermi Model

Since it is likely that the optimum value of γ will turn out to be moderate, it may be sufficient for a less refined analysis to set it to zero exactly. The result is a considerable simplification in the energy equations and the Euler equations. Similarly, the potential felt by a nucleon in standard nuclear matter could then be simply expressed as

$$u(\phi) = -\alpha + \frac{3}{5}\beta + \frac{4}{3}\sigma + \beta\phi^2 \,. \tag{54}$$

This implies a constant effective mass m^* for the nucleon, given by $m^*/m = (1+\beta)^{-1}$. The older (Seyler-Blanchard) model without a density dependent term (i.e. with $\sigma = 0$) would require β to be about 1.6, leading to the unacceptable value $m^*/m = 0.38$. With the σ term included, β is close to 0.4, which gives $m^*/m = 0.71$. This value reproduces adequately the trend of the experimental data in Fig. 8 concerning the depths of the optical model potentials. Thus, using the saturation equations (20,21) with γ put equal to zero, and writing $\phi^2 = \varepsilon - u$, we find for the potential u the simple expression

$$u = -1 + \frac{\eta_o}{1+\beta} + \frac{\beta}{1+\beta}\varepsilon \,, \tag{55}$$

or, equivalently (after restoring the units),

$$U(E) = -T_o - \frac{a_1}{1+\beta} + \frac{\beta}{1+\beta}E \,. \tag{56}$$

With γ set equal to zero a preliminary fit of the remaining parameters to nuclear masses (and to the theoretical estimate of neutron matter [14]) results in the following slightly modified illustrative parameter set:

$$\begin{aligned} a &= 0.58820 \text{ fm}, \\ \alpha &= 3.99474, \quad \beta = 0.38096, \quad \gamma = 0.0, \\ \sigma &= 1.45969, \quad \xi = 0.44308, \quad \zeta = 0.57047 \,. \end{aligned} \tag{57}$$

These values correspond to the following nuclear properties:

$$\begin{aligned} &\text{radius constant of nuclear matter,} && r_o = 1.13 \text{ fm}, \\ &\text{Fermi energy of nuclear matter,} && T_o = 37.679 \text{ MeV}, \\ &\text{density of nuclear matter,} && \rho = 0.16545 \text{ fm}^{-3}, \\ &\text{volume energy coefficient,} && a_1 = 16.539 \text{ MeV}, \\ &\text{symmetry energy coefficient,} && J = 31.633 \text{ MeV}, \\ &\text{surface energy coefficient,} && a_2 = 20.237 \text{ MeV}, \\ &\text{curvature correction coefficient,} && a_3 = 10.432 \text{ MeV}, \\ &\text{compressibility coefficient,} && K = 315.91 \text{ MeV}. \end{aligned} \tag{58}$$

The depth of the optical model potential in Fig. 8 is now strictly linear in the energy E and changes sign at $E = 180$ MeV.

The actual expression used for the nuclear mass excess in the determination of this preliminary (and truncated) parameter set, was

$$M(N,Z) = M_N N + M_H Z + TF + a_0 + W|I| + EO + SH \ , \qquad (59)$$

where N is the number of neutrons, Z the number of protons and $I = (N-Z)/(N+Z)$. The coefficients are:

$$\begin{array}{lrcl} \text{mass excess of the neutron,} & M_N & = & 8.071431 \text{ MeV,} \\ \text{mass excess of the hydrogen atom,} & M_H & = & 7.289034 \text{ MeV,} \\ \text{constant term,} & a_0 & = & -16.7710 \text{ MeV,} \\ \text{Wigner term coefficient,} & W & = & 30.0 \text{ MeV.} \end{array} \qquad (60)$$

and TF is the Thomas-Fermi calculation of the binding energy (a negative number). The even-odd correction EO has the form:

$$EO = \begin{cases} 0 & \text{for even-even nuclei,} \\ 12/\sqrt{A} & \text{for odd nuclei,} \\ 24/\sqrt{A} - 20/A & \text{for odd-odd nuclei.} \end{cases} \qquad (61)$$

The fit was performed by Peter Möller [22] using 335 masses and the shell corrections SH from Ref.[23]. The rms deviation of the measured and calculated masses for the nuclei used in the fit was 0.958 MeV.

11 Summary and Outlook

We have presented a model of average nuclear properties based on a Thomas-Fermi theory with an effective interaction that contains seven parameters. These consist of the usual four basic parameters determined by nuclear sizes and by the nuclear volume, surface and symmetry energies, plus a fifth parameter γ determined by the nuclear surface diffuseness, plus a sixth parameter that can be adjusted to (theoretical) estimates of the properties of neutron matter, plus a seventh parameter σ, determined by the energy dependence of the nuclear optical potential. The number of parameters is in a very healthy relation to the amount of data used to fit them, and this results in a phenomenological model for the most part firmly anchored in observable properties of nuclei. The formal structure of the model is such that, apart only from shell effects and the discreteness of nucleons, there are no reasons to doubt its validity for small nuclei, or its powers of extrapolation to very large, or very deformed, or very neutron or proton rich systems. Thus we picture ourselves in possession of a reliable approximation to the average properties of the matter of which nuclei are composed. In order to exploit this situation fully, we are planning, in addition to a large number of conven-

tional applications, to subject droplets of our Thomas-Fermi nuclear matter to a range of extreme conditions. These will include large centrifugal forces, extreme electric forces (associated with huge atomic numbers), as well as stresses produced by extreme isospin imbalance and high temperatures [24]. It is known that under such extreme conditions nuclei have a tendency to assume unusual shapes such as dumbbells, bubbles, or tori, not to mention the "spaghetti", "lasagna" etc. configurations contemplated in astrophysical applications [25,26]. The availability of a reliable statistical model of the nuclear material is essential for extrapolating into those exotic regimes of nuclear physics.

12 Appendix A. The Interaction Energy

The interaction energy W is the sum of neutron-neutron, neutron-proton and proton-proton interaction energies: $W = W_{nn} + W_{np} + W_{pp}$, where

$$W_{nn\,\mathrm{or}\,pp} = -\frac{1}{2}\int d^3r_1 \int d^3r_2 \int_{n\,\mathrm{or}\,p} d^3p_1 \int_{n\,\mathrm{or}\,p} d^3p_2 (2/h^3) C_\ell f\,,$$

$$W_{np} = -\int d^3r_1 \int d^3r_2 \int_{neutrons} d^3p_1 \int_{protons} d^3p_2 (2/h^3) C_u f\,. \quad (62)$$

In the above, the first two integrations are over all space, and the momentum integrations are over the Fermi spheres of radius P_1 and P_2 associated with the interacting particles (neutrons or protons) at points 1 and 2. The factor $2/h^3$ is the density of neutron or proton states in phase space and C_ℓ and C_u stand for the interaction strengths between like and unlike particles. Using the dimensionless quantities defined in Sec. 2 we find for W_{nn}, say, the expression

$$W_{nn} = -\frac{1}{2} T_o\,(\rho_o/2) \int d^3r_1 \int d^3r_2 f\,(\alpha_\ell I_1 - \beta_\ell I_2 + \gamma_\ell I_3 - \sigma_\ell I_4)\,, \quad (63)$$

where the I's are the following momentum integrals:

$$I_1\,(\Phi_1, \Phi_2) = \left(\frac{4}{3}\pi P_o^3\right)^{-2} \int_{P_1} d^3p_1 \int_{P_2} d^3p_2 = \Phi_1^3 \Phi_2^3$$

$$
\begin{aligned}
I_2(\Phi_1,\Phi_2) &= \left(\frac{4}{3}\pi P_o^3\right)^{-2}\int_{P_1} d^3p_1 \int_{P_2} d^3p_2 (p_{12}/P_o)^2 \qquad (64)\\
I_3(\Phi_1,\Phi_2) &= \left(\frac{4}{3}\pi P_o^3\right)^{-2}\int_{P_1} d^3p_1 \int_{P_2} d^3p_2 (P_o/p_{12})\\
I_4(\Phi_1,\Phi_2) &= \left(\frac{4}{3}\pi P_o^3\right)^{-2}\frac{1}{2}\left(\Phi_1^2+\Phi_2^2\right)\int_{P_1} d^3p_1 \int_{P_2} d^3p_2\\
&= \frac{1}{2}\left(\Phi_1^2+\Phi_2^2\right)\Phi_1^3\Phi_2^3
\end{aligned}
$$

Analogous expressions hold for W_{np} and W_{pp}, with $I_i(\Phi_1,\Phi_2)$ replaced by $I_i(\Phi_1,\Psi_2)$ and $I_i(\Psi_1,\Psi_2)$, respectively. For example,

$$
\begin{aligned}
I_4(\Phi_1,\Psi_2) &= \frac{1}{2}\left(\Phi_1^2+\Psi_2^2\right)\Phi_1^3\Psi_2^3 \qquad (65)\\
I_4(\Psi_1,\Psi_2) &= \frac{1}{2}\left(\Psi_1^2+\Psi_2^2\right)\Psi_1^3\Psi_2^3 .
\end{aligned}
$$

We shall presently return to evaluating I_2 and I_3, but first consider the contribution W_σ to the energy W, arising from the density dependent σ-term in the interaction:

$$
\begin{aligned}
W_\sigma &= \frac{1}{2}T_o(\rho_o/2)\int d^3r_1\int d^3r_2 f\left[\sigma_\ell I_4(\Phi_1,\Phi_2)+\sigma_\ell I_4(\Psi_1,\Psi_2)+2\sigma_u I_4(\Phi_1,\Psi_2)\right]\\
&= \frac{1}{2}T_o(\rho_o/2)\int d^3r_1\int d^3r_2 f\left[\frac{1}{2}\sigma_\ell\left(\Phi_1^5\Phi_2^3+\Phi_1^3\Phi_2^5+\Psi_1^5\Psi_2^3+\Psi_1^3\Psi_2^5\right)\right.\\
&\qquad\qquad \left.+\,\sigma_u\left(\Phi_1^5\Psi_2^3+\Phi_1^3\Psi_2^5\right)\right]. \qquad (66)
\end{aligned}
$$

Since the indices 1 and 2 in the integration variables may be interchanged at will, the above reduces to

$$W_\sigma = \tag{67}$$
$$\frac{1}{2}T_o(\rho_o/2)\int d^3r_1\int d^3r_2 f\left[\sigma_\ell\left(\Phi_1^5\Phi_2^3+\Psi_1^5\Psi_2^3\right)+\sigma_u\left(\Phi_1^5\Psi_2^3+\Phi_1^3\Psi_2^5\right)\right].$$

We shall also need an expression for the contribution from the σ-term to the *potential* felt by a neutron (or proton). This is obtained by imagining the neutron density ρ_n changed to $\rho_n+\delta\rho_n$, calculating the resulting change δW_σ, and casting it in the form

$$\delta W_\sigma = \int d^3r_1 U_\sigma(r_1)\,\delta\rho_n(1)\,, \tag{68}$$

so that $U_\sigma(r_1)$ is the desired potential. Carrying out the variations $\Phi_1\rightarrow\Phi_1+\delta\Phi_1$ and $\Phi_2\rightarrow\Phi_2+\delta\Phi_2$ in Eq.(76), interchanging indices 1 and 2 where necessary in order to convert $\delta\Phi_2$ into $\delta\Phi_1$, and using $\delta\rho_n(1)=(\rho_o/2)3\Phi_1^2\,\delta\Phi_1$, we find

$$U_\sigma \;=\; T_o\int d^3r_2 f\left[\sigma_\ell\left(\frac{5}{6}\Phi_1^2\Phi_2^3+\frac{1}{2}\Phi_2^5\right)+\sigma_u\left(\frac{5}{6}\Phi_1^2\Psi_2^3+\frac{1}{2}\Psi_2^5\right)\right]. \tag{69}$$

The corresponding expression for the potential felt by a proton is obtained by interchanging Φ and Ψ.

The potential produced by the density-independent part of the interaction can be obtained more directly by integrating over contributions from the particles surrounding a given "test particle", or "test density" $\delta\rho$. (This cannot be done for the density-dependent part because the introduction of the test density affects the interactions between all the particles already present, and this contributes to the energy change and thus to the effective potential. This is why we had to deduce U_σ by first calculating W_σ, and then evaluating the variation δW_σ. If this subtle point is disregarded, an incorrect expression for U_σ is obtained.)

The total potential felt by a neutron at the point r_1 and with momentum p can now be written as,

$$\begin{aligned} U_n(r_1,p) = U_\sigma(r_1) \quad &- \quad T_o \int d^3r_2 f\left(\alpha_\ell i_1 - \beta_\ell i_2 + \gamma_\ell i_3\right) \\ &- \quad T_o \int d^3r_2 f\left(\alpha_u i_1 - \beta_u i_2 + \gamma_u i_3\right) , \end{aligned} \tag{70}$$

where, for neutron-neutron interactions, the i's are the following momentum integrals:

$$\begin{aligned} i_1(\Phi_2) &= \left(\frac{4}{3}\pi P_o^3\right)^{-1} \int_{P_2} d^3p_2 = \Phi_2^3 \\ i_2(\Phi_2,p) &= \left(\frac{4}{3}\pi P_o^3\right)^{-1} \int_{P_2} d^3p_2 (p_{12}/P_o)^2 \end{aligned} \tag{71}$$

$$i_3(\Phi_2, p) \;=\; \left(\frac{4}{3}\pi P_o^3\right)^{-1} \int_{P_2} d^3p_2 (P_o/p_{12})\,.$$

In the case of neutron-proton interactions Φ is replaced by Ψ.

The integral i_2 is evaluated by writing

SEE LBL 30395

$$p_{12}^2 = p_x^2 + p_y^2 + (p_z - p)^2\,, \tag{72}$$

where p_x, p_y, p_z are the cartesian components of $\mathbf{p}_2$, and by choosing the vector $\mathbf{p}_1$, whose magnitude is p, to lie along the p_z axis. Thus,

$$i_2 = \left(\frac{4}{3}\pi P_o^3\right)^{-1} P_o^{-2} \int_{P_2} d^3p_2 (p_2^2 - 2p_z p + p^2)\,. \tag{73}$$

The integration over p_z vanishes by symmetry, and we find

$$\begin{aligned} i_2 &= (P_2/P_o)^3 P_o^{-2} \left(\frac{3}{5}P_2^2 + p\right) \\ &= \Phi_2^3 \left(\frac{3}{5}\Phi_2^2 + \phi^2\right)\,, \end{aligned} \tag{74}$$

where ϕ, equal to p/P_o, is the neutron's momentum in units of the Fermi momentum P_o.

In the case of i_3 we make use of the fact that $\int_{P_2} d^3p_2/p_{12}$ may be regarded as a fictitious electric potential (in momentum space) at a distance p from the origin, due to a uniform distribution of charge inside the sphere P_2. Using

standard formulae of electrostatics, we have

$$i_3 = \begin{cases} \Phi_2^3\,\phi^{-1} & \text{, if } \phi > \Phi_2 \\ \Phi_2^2\left[\frac{3}{2} - \frac{1}{2}(\phi/\Phi_2)^2\right] & \text{, if } \phi < \Phi_2\,. \end{cases} \tag{75}$$

The contributions to U_n from the protons are obtained by replacing Φ by Ψ.

The total potential felt by a neutron is given by:

$$U_n(r_1,\phi) = \tag{76}$$

$$-T_o \int d^3r_2\, f\, \Phi_2^3 \left\{ \alpha_\ell - \beta_\ell\left(\frac{3}{5}\Phi_2^2 + \phi^2\right) - \sigma_\ell\left(\frac{5}{6}\Phi_1^2 + \frac{1}{2}\Phi_2^2\right) + \gamma_\ell \begin{cases} \phi^{-1} \\ \Phi_2^{-1}\left[\frac{3}{2} - \frac{1}{2}(\phi/\Phi_2)^2\right] \end{cases} \right\}$$

$$-T_o \int d^3r_2\, f\, \Psi_2^3 \left\{ \alpha_u - \beta_u\left(\frac{3}{5}\Psi_2^2 + \phi^2\right) - \sigma_u\left(\frac{5}{6}\Phi_1^2 + \frac{1}{2}\Psi_2^2\right) + \gamma_u \begin{cases} \phi^{-1} \\ \Psi_2^{-1}\left[\frac{3}{2} - \frac{1}{2}(\phi/\Psi_2)^2\right] \end{cases} \right\}.$$

In the factors multiplying γ, the lower line is to be used when $\phi < \Phi_2$ or Ψ_2 respectively, and the upper line otherwise. The proton potential $U_p(r_1,\psi)$ is obtained by interchanging Φ and Ψ, and adding the electric potential:

$$U_p(r_1,\psi) = \tag{77}$$

$$-T_o \int d^3r_2\, f\, \Psi_2^3 \left\{ \alpha_\ell - \beta_\ell\left(\frac{3}{5}\Psi_2^2 + \psi^2\right) - \sigma_\ell\left(\frac{5}{6}\Psi_1^2 + \frac{1}{2}\Psi_2^2\right) + \gamma_\ell \begin{cases} \psi^{-1} \\ \Psi_2^{-1}\left[\frac{3}{2} - \frac{1}{2}(\psi/\Psi_2)^2\right] \end{cases} \right\}$$

$$-T_o \int d^3r_2\, f\, \Phi_2^3 \left\{ \alpha_u - \beta_u\left(\frac{3}{5}\Phi_2^2 + \psi^2\right) - \sigma_u\left(\frac{5}{6}\Psi_1^2 + \frac{1}{2}\Phi_2^2\right) + \gamma_u \begin{cases} \psi^{-1} \\ \Phi_2^{-1}\left[\frac{3}{2} - \frac{1}{2}(\psi/\Phi_2)^2\right] \end{cases} \right\}$$

$$+ e^2(\rho_o/2) \int d^3r_2\, \Psi_2^3/r_{12}\,.$$

In the above, ψ is the proton's momentum in units of P_o.

Note that for a neutron "at the top of its Fermi sphere", i.e. for $\phi = \Phi_1$ the neutron potential becomes,

$$U_n(r_1, \Phi_1) = \tag{78}$$

$$-T_o \int d^3r_2\, f \left[\Phi_2^3 \left\{ \alpha_\ell - B_\ell \left(\frac{3}{5}\Phi_2^2 + \Phi_1^2 \right) + \gamma_\ell \left\langle \begin{array}{l} \Phi_1^{-1} \\ \Phi_2^{-1} \left[\frac{3}{2} - \frac{1}{2}(\Phi_1/\Phi_2)^2 \right] \end{array} \right. \right\} \right.$$

$$\left. + \Psi_2^3 \left\{ \alpha_u - B_u \left(\frac{3}{5}\Psi_2^2 + \Phi_1^2 \right) + \gamma_u \left\langle \begin{array}{l} \Phi_1^{-1} \\ \Psi_2^{-1} \left[\frac{3}{2} - \frac{1}{2}(\Phi_1/\Psi_2)^2 \right] \end{array} \right. \right\} \right] .$$

Similarly, for a proton with $\psi = \Psi_1$, we have (apart from the electric potential),

$$U_p(r_1, \Psi_1) = \tag{79}$$

$$-T_o \int d^3r_2\, f \left[\Psi_2^3 \left\{ \alpha_\ell - B_\ell \left(\frac{3}{5}\Psi_2^2 + \Psi_1^2 \right) + \gamma_\ell \left\langle \begin{array}{l} \Psi_1^{-1} \\ \Psi_2^{-1} \left[\frac{3}{2} - \frac{1}{2}(\Psi_1/\Psi_2)^2 \right] \end{array} \right. \right\} \right.$$

$$\left. + \Phi_2^3 \left\{ \alpha_u - B_u \left(\frac{3}{5}\Phi_2^2 + \Psi_1^2 \right) + \gamma_u \left\langle \begin{array}{l} \Psi_1^{-1} \\ \Phi_2^{-1} \left[\frac{3}{2} - \frac{1}{2}(\Psi_1/\Phi_2)^2 \right] \end{array} \right. \right\} \right] .$$

The noteworthy feature of Eqs.(80) and (81) is that only the combinations of β and σ denoted by B are in evidence.

Returning now to the calculation of the interaction energy W in Eqs.(62,63), the integrals $I_1(\Phi_1, \Phi_2)$, $I_1(\Phi_1, \Psi_2)$, $I_1(\Psi_1, \Psi_2)$ are trivially evaluated as $\Phi_1^3\Phi_2^3$, $\Phi_1^3\Psi_2^3$, $\Psi_1^3\Psi_2^3$. The quantity $I_2(\Phi_1, \Phi_2)$ involves integrating i_2 over the sphere P_1. Since the average of ϕ^2 over this sphere if $\frac{3}{5}\Phi_1^2$, we find at once that,

$$\begin{aligned} I_2(\Phi_1, \Phi_2) &= \frac{3}{5}\Phi_1^3\Phi_2^3(\Phi_1^2 + \Phi_2^2) = \frac{6}{5}I_4(\Phi_1, \Phi_2) \\ I_2(\Phi_1, \Psi_2) &= \frac{3}{5}\Phi_1^3\Psi_2^3(\Phi_1^2 + \Psi_2^2) = \frac{6}{5}I_4(\Phi_1, \Psi_2) \\ I_2(\Psi_1, \Psi_2) &= \frac{3}{5}\Psi_1^3\Psi_2^3(\Psi_1^2 + \Psi_2^2) = \frac{6}{5}I_4(\Psi_1, \Psi_2)\,. \end{aligned} \tag{80}$$

Finally, $I_3(\Phi_1, \Phi_2)$ involves an integration of i_3 over the sphere P_1. Here we have to make a distinction between the case when $\Phi_1 > \Phi_2$ and $\Phi_1 < \Phi_2$. In the latter case ϕ, which is less than Φ_1, is always less than Φ_2, and the lower line in Eq.(75)is to be used. As before, the average of ϕ^2 over the sphere P_1 is $\frac{3}{5}\Phi_1^2$ and we find

$$I_3(\Phi_1, \Phi_2) = \Phi_1^3\Phi_2^3\,\Phi_2^{-1}\,\frac{3}{2}\left[1 - \frac{1}{5}(\Phi_1/\Phi_2)^2\right]\,, \text{ for } \Phi_1 < \Phi_2\,. \tag{81}$$

When $\Phi_1 > \Phi_2$, ϕ is sometimes less and sometimes greater than Φ_2. Hence the somewhat more complicated integral:

$$\begin{aligned} I_3(\Phi_1, \Phi_2) &= \Phi_1^3\Phi_2^3\left\{\int_0^{\Phi_2} d\phi\phi^2\,\Phi_2^{-1}\left[\frac{3}{2} - \frac{1}{2}(\phi/\Phi_2)^2\right] + \int_{\Phi_2}^{\Phi_1} d\phi\phi^2\,\phi^{-1}\right\}\Big/\int_0^{\Phi_1} d\phi\phi^2 \\ &= \Phi_1^3\Phi_2^3\,\Phi_1^{-1}\,\frac{3}{2}\left[1 - \frac{1}{5}(\Phi_2/\Phi_1)^2\right]\,, \text{ for } \Phi_1 > \Phi_2\,. \end{aligned} \tag{82}$$

Both final results for I_3 are nevertheless symmetric in Φ_1, Φ_2 and may be summarized by writing

$$I_3(\Phi_1, \Phi_2) = \Phi_1^3 \Phi_2^3 \Phi_>^{-1} \frac{3}{2} \left[1 - \frac{1}{5} (\Phi_< / \Phi_>)^2 \right] , \tag{83}$$

where $\Phi_<$, $\Phi_>$ is the lesser or greater of Φ_1 and Φ_2. Similarly,

$$I_3(\Psi_1, \Psi_2) = \Psi_1^3 \Psi_2^3 \Psi_>^{-1} \frac{3}{2} \left[1 - \frac{1}{5} (\Psi_< / \Psi_>)^2 \right] , \tag{84}$$

and

$$I_3(\Phi_1, \Psi_2) = \Phi_1^3 \Psi_2^3 X_>^{-1} \frac{3}{2} \left[1 - \frac{1}{5} (X_< / X_>)^2 \right] , \tag{85}$$

where $X_<$, $X_>$ is the lesser or greater of Φ_1 and Ψ_2.

Collecting together all contributions we find,

$$\begin{aligned}
W_{nn} &= -\frac{1}{2} T_o (\rho_o/2) \int d^3 r_1 \int d^3 r_2 \, f \, \Phi_1^3 \Phi_2^3 \left\{ \alpha_\ell - \frac{6}{5} B_\ell \Phi_1^2 + \frac{3}{2} \gamma_\ell \Phi_>^{-1} \left[1 - \frac{1}{5} (\Phi_< / \Phi_>)^2 \right] \right\} , \\
W_{pp} &= -\frac{1}{2} T_o (\rho_o/2) \int d^3 r_1 \int d^3 r_2 \, f \, \Psi_1^3 \Psi_2^3 \left\{ \alpha_\ell - \frac{6}{5} B_\ell \Psi_1^2 + \frac{3}{2} \gamma_\ell \Psi_>^{-1} \left[1 - \frac{1}{5} (\Psi_< / \Psi_>)^2 \right] \right\} , \\
W_{np} &= -\frac{1}{2} T_o (\rho_o/2) \int d^3 r_1 \int d^3 r_2 \, f \, \Phi_1^3 \Psi_2^3 \left\{ \alpha_u - \frac{3}{5} B_u (\Phi_1^2 + \Psi_2^2) + \frac{3}{2} \gamma_\ell X_>^{-1} \left[1 - \frac{1}{5} (X_< / X_>)^2 \right] \right\} .
\end{aligned} \tag{86}$$

13 Appendix B. Numerical Solution of the Euler Equations.

The Euler Equations consist of a pair of coupled integral equations for Φ and Ψ, viz.:

$$\begin{aligned} \Phi^3 - C_1^{\mathrm{n}}\Phi - C_0^{\mathrm{n}} &= 0 \\ \Psi^3 - C_1^{\mathrm{p}}\Psi - C_0^{\mathrm{p}} &= 0\,, \end{aligned} \tag{87}$$

where the coefficients C are functionals of Φ and Ψ given by Eqs.(32).

The following procedure was found to lead to convergent iterative numerical solutions. Assuming starting estimates for Φ and Ψ and for the chemical potentials Λ_n and Λ_p, the coefficients $C_0^{\mathrm{n,p}}$, $C_1^{\mathrm{n,p}}$ are calculated by numerically integrating Eqs.(32). The cubic equations (87) are then solved for Φ and Ψ. The associated density distributions are integrated to determine the number of neutrons and protons, and the chemical potentials are adjusted until the neutron and proton numbers agree with those implied by the initial choice of Φ and Ψ. The new functions Φ and Ψ thus obtained constitute the next approximation to the desired solutions. The integrations in Eqs.(32) are performed again and the whole procedure is iterated to convergence, usually

in about 8 to 10 steps.

In solving the cubic equations, the following formulae were found appropriate (X stands for Φ or Ψ and C stands for C^{n} orC^{p}):

If the discriminant $b \equiv \frac{1}{4}C_0^2 - \frac{1}{27}C_1^3 > 0$, then

$$X = \left(\frac{1}{2}C_0 + \sqrt{b}\right)^{1/3} + \left(\frac{1}{2}C_0 - \sqrt{b}\right)^{1/3} . \tag{88}$$

If $b < 0$, then

$$X = 2\sqrt{C_1/3}\,\cos\left[\frac{1}{3}\cos^{-1}\sqrt{1 + 27b/C_1^3}\right] . \tag{89}$$

14 Appendix C. Relation to Droplet Model Coefficients

The energy per particle of uniform nuclear matter, Eq.(25), has the following expansion around its equilibrium value,

$$\eta = \eta_0 + (\omega_0\varepsilon + \omega_1\delta^2) + \frac{1}{2}(\omega_2\varepsilon^2 - 2\omega_3\varepsilon\delta^2 + \omega_4\delta^4) - \omega_5|\delta|^3 - \omega_6|\delta|^5 + \cdots \,. \quad (90)$$

Here ε is the Droplet Model dilatation variable, defined by

$$\rho/\rho_o = 1 - 3\varepsilon \,, \quad (91)$$

where ρ is the total density, $\rho_{\rm n} + \rho_{\rm p}$, and δ is the relative neutron excess variable defined by $\delta = (\rho_{\rm n} + \rho_{\rm p})/\rho$. The expansion coefficients ω_i are found to be the following functions of the interaction parameters α, β etc.:

$$\begin{aligned}
\eta_0 &= \frac{3}{5} - \frac{1}{2}\alpha + \frac{3}{5}B - \frac{3}{5}\gamma \,, \\
\omega_0 &= -\frac{6}{5} + \frac{3}{2}\alpha - 3B + \frac{6}{5}\gamma \,, \\
\omega_1 &= \frac{1}{3} - \frac{1}{2}\alpha_\ell + \frac{1}{2}\alpha_u + \frac{4}{3}B_\ell - \frac{2}{3}B_u - \frac{1}{3}\gamma_\ell + \frac{2}{3}\gamma_u \,, \\
\omega_2 &= \frac{6}{5} - 3\alpha + 12B - \frac{6}{5}\gamma \\
\omega_3 &= \frac{2}{3} - \frac{3}{2}\alpha_\ell + \frac{3}{2}\alpha_u + \frac{20}{3}B_\ell - \frac{10}{3}B_u - \frac{2}{3}\gamma_\ell + \frac{4}{3}\gamma_u \,, \\
\omega_4 &= \frac{2}{81} - \frac{4}{81}B_\ell + \frac{8}{81}B_u - \frac{2}{81}\gamma_\ell + \frac{10}{81}\gamma_u \,,
\end{aligned} \quad (92)$$

$$\omega_5 = \frac{1}{9}\gamma_u\,,$$
$$\omega_6 = \frac{14}{405}\gamma_u\,.$$

The Droplet Model coefficients a_1, J, K, L, M are related to the ω's by the expressions,

$$a_1 = -\eta_0\,T_o\,,\ J = \omega_1\,T_o\,,\ K = \omega_2\,T_o\,,\ L = \omega_3\,T_o\,,\ M = \omega_4\,T_o\,. \tag{93}$$

The terms in $\omega_5|\delta^3|$, $\omega_6|\delta^5|$, absent in the Droplet Model, are the result of the non-analytic behavior associated with the term γp_{12}^{-1} in the effective interaction.

15 Acknowledgements

The authors wish to acknowledge discussions with P. Möller and J. Randrup, and the substantial contributions that P. Möller made by determining the model parameters from a fit of the calculated binding energies to the measured masses of nuclei.

References

[1] W.D. Myers and W.J. Swiatecki, Ann. Rev. Nucl. Part. Phys. **32** (1982) 309.

[2] W.D. Myers and W. J. Swiatecki, Ann. Phys. (N. Y.) **55** (1969) 395.

[3] W.D. Myers, Droplet model of atomic nuclei (IFI/Plenum, New York, 1977).

[4] W.D. Myers, Proc. Third Intl. Conf. on Atomic Masses, R.C. Barber Editor, Winnipeg, Canada, 28 Aug.- 1 Sep., 1967, p.61-84.

[5] M. Brack, C. Guet and H.-B. Hakansson, Phys. Rep. **123** (1985) 275-364.

[6] A.K. Dutta, J.-P. Arcoragi, J.M.Pearson, R. Behrman and F. Tondeur, Nucl. Phys. **A458** (1986) 77-94.

[7] F. Tondeur, A.K. Dutta, J.M. Pearson and R. Behrman, Nucl. Phys. **A470** (1987) 93-106.

[8] R.G. Seyler and C.H. Blanchard, Phys. Rev. **124**, 227 (1961); **131** (1963) 355.

[9] H. von Groote, Proc. 3rd Int. Conf. on nuclei far from stability, ed. R. Klapisch, CERN 76-13 p. 595 (1976).

[10] W.D. Myers, The Proceedings of the Gross Properties of Nuclei and Nuclear Excitations International Workshop XVIII, Hirschegg, Austria,15-20 January 1990.

[11] D. Bandyopadhyay and S.K. Samaddar, Nucl. Phys. **A484** (1988) 315.

[12] W.J. Swiatecki, Proc. Phys. Soc. (London) **A68** (1955) 285.

[13] H.A. Bethe, Phys. Rev. **167** (1968) 879.

[14] B. Friedman and V.R. Pandharipande, Nucl. Phys. **A361** (1981) 502.

[15] C. Samanta, D. Bandyopadhyay, and J.N. De, Phys. Lett. **B217** (1989) 381.

[16] H. de Vries, C.W. Jager and C. de Vries, At. Data Nucl. Data Tables **36** (1987) 495-536.

[17] M. Bauer, E. Hernández-Saldaña, P.E. Hodgson and J. Quintanilla, J. Phys. G: Nucl. Phys. **8** (1982) 525-34.

[18] W.D. Myers, Nucl. Phys. **A145** (1970) 387-400.

[19] A. Bohr and B.R. Mottelson, "Nuclear Structure" Vol. 2, W.A. Benjamin Inc., 1975.

[20] P. Möller, private communication, November 1989.

[21] G. Süssmann, Z. Phys. **A274** (1975) 145-59.

[22] P. Möller, private communication, March 1990.

[23] P. Möller and J. R. Nix, At. Data Nucl. Data Tables **26** (1981) 165.

[24] J. Randrup and Emil de Lima Medeiros, Lawrence Berkeley Laboratory Report, LBL-28797, March, 1990.

[25] D.G. Ravenhall, C.J. Pethick and J.R. Wilson, Phys. Rev. Lett. **50** (1983) 2066.

[26] R.D. Williams and S.E. Koonin, Nucl. Phys. **A435** (1985) 844.

Figure Captions

Fig. 1 The binding energy per particle of standard nuclear matter (in units of T_o) as a function of Ω, the Fermi momentum in units of P_o. (The relative density ρ/ρ_o is equal to Ω^3.) The compressibility $K = 300$ MeV is approximately the value we have deduced from experiment. The value $K = 10,000$ illustrates the approach of our model to the limiting case of an incompressible liquid drop.

Fig. 2 The energy per particle of uniform nuclear matter (in units of T_o) for different values of the relative neutron excess $\delta = (\rho_n - \rho_p)/(\rho_n + \rho_p)$. The parameter Γ is related to the relative density by $\Gamma^3 \equiv \rho/\rho_o$. Neutron matter corresponds to $\delta = 1$ and is given by the upper solid curve. Neutron matter at a density equal to the neutron density prevailing in equilibrium standard nuclear matter (i.e. $\rho_n = \rho_o/2$) corresponds to $\Gamma = (1/2)^{1/3} = 0.7937$. Up to such a density the solid curve agrees closely with the theoretical estimate of Ref.[14], given by the squares.

Fig. 3 The energy per particle of neutron matter (in units of T_o), for various values of the parameter ξ, which is a measure of the relative strength of interactions between like and unlike particles. The cube of the parameter

Φ is the neutron matter density in units of $\rho_o/2$. For each value of ξ the other interaction parameters were readjusted so as to keep the binding, density and symmetry energy coefficient of standard nuclear matter fixed. For a value of ξ equal to about 0.44 the Thomas-Fermi calculation agrees closely (up to $\Phi \approx 1$) with the estimates of Ref.[14], given by the squares. For ξ less than about 0.2, the energy plot develops a metastable minimum, which becomes stable for ξ less than about -0.1.

Fig. 4 The calculated Thomas-Fermi charge distribution of three nuclei (after folding in the proton size) are compared with experimental distributions represented by a so-called 3-parameter Gaussian fit [16]. The RMS radii of the calculated and measured distributions are about equal. A better fit could have been obtained by increasing the calculated surface diffuseness (resulting in a reduction of the compressibility coefficient).

Fig. 5 The calculated Thomas-Fermi density profile of standard, semi-infinite nuclear matter is shown by the solid curve. The dashed line is the result of folding in a Yukawa nucleon form factor with an RMS size of 0.85 fm, corresponding to the measured charge distribution of a proton. The distance along the abscissa is measured from the location of the effective sharp surface.

Fig. 6 Each set of symbols represents the result of calculating the surface energy of semi-infinite nuclear matter using interaction parameters chosen so as to give the same volume energy per particle, the same equilibrium density and the same surface width b, but different compressibility coefficients K. The value of b deduced from measured charge distributions ($b \approx 1$ fm), together with the value of a_2 deduced from fits to measured binding energies ($a_2 \approx 20$ MeV), leads to an estimated value for K of about 300 MeV. (Some evidence for a value of b greater than 1 fm is suggested by Fig. 4.) Note the astonishingly linear appearance of the graph resulting from plotting a_2 vs. K at fixed b. (The lines are straight line fits to the calculated points.)

Fig. 7 The calculated momentum dependence of the potential felt by a neutron traveling through standard nuclear matter. (The potential is in units of T_o and the momentum is in units of P_o). The total potential (solid curve) is made up of a negative constant (long dashes), plus the parabolic term $\beta\phi^2$ (medium dashes) and the γ-term proportional to ϕ^2 for $\gamma < 1$, and to ϕ^{-1} for $\gamma > 1$ (short dashes).

Fig. 8 A compilation of the measurements of the depth of the optical model potential, taken from Ref.[17], is compared with the Thomas-Fermi calculations. The short-dashed line would be the result of using the original

Seyler-Blanchard model [8] with $\gamma = 0$ and $\sigma = 0$. Increasing σ to 1.33677 gives the dotted line (and the same compressibility). Taking γ to have the value which reproduces approximately the measured surface diffuseness ($\gamma = 0.21329$) bends the curve up away from the abscissa to give the solid curve. (The compressibility is now $K = 301.27$ MeV.) All the curves pass through the fixed point at $U = -54.206$ MeV, $E = -16.527$ MeV and are strictly linear and independent of γ for $E < -16.527$ MeV. The long-dashed line results from increasing the value of γ to 0.45305, which corresponds to $K =$ 285

LAWRENCE BERKELEY LABORATORY
UNIVERSITY OF CALIFORNIA
INFORMATION RESOURCES DEPARTMENT
BERKELEY, CALIFORNIA 94720